NASA/TP-2006-213676

Extended Aging Theories for Predictions of Safe Operational Life of Critical Airborne Structural Components

William L. Ko and Tony Chen
NASA Dryden Flight Research Center
Edwards, California

May 2006

NASA STI Program ... in Profile

Since its founding, NASA has been dedicated to the advancement of aeronautics and space science. The NASA scientific and technical information (STI) program plays a key part in helping NASA maintain this important role.

The NASA STI program is operated under the auspices of the Agency Chief Information Officer. It collects, organizes, provides for archiving, and disseminates NASA's STI. The NASA STI program provides access to the NASA Aeronautics and Space Database and its public interface, the NASA Technical Report Server, thus providing one of the largest collections of aeronautical and space science STI in the world. Results are published in both non-NASA channels and by NASA in the NASA STI Report Series, which includes the following report types:

- TECHNICAL PUBLICATION. Reports of completed research or a major significant phase of research that present the results of NASA programs and include extensive data or theoretical analysis. Includes compilations of significant scientific and technical data and information deemed to be of continuing reference value. NASA counterpart of peer-reviewed formal professional papers but has less stringent limitations on manuscript length and extent of graphic presentations.

- TECHNICAL MEMORANDUM. Scientific and technical findings that are preliminary or of specialized interest, e.g., quick release reports, working papers, and bibliographies that contain minimal annotation. Does not contain extensive analysis.

- CONTRACTOR REPORT. Scientific and technical findings by NASA-sponsored contractors and grantees.

- CONFERENCE PUBLICATION. Collected papers from scientific and technical conferences, symposia, seminars, or other meetings sponsored or cosponsored by NASA.

- SPECIAL PUBLICATION. Scientific, technical, or historical information from NASA programs, projects, and missions, often concerned with subjects having substantial public interest.

- TECHNICAL TRANSLATION. English-language translations of foreign scientific and technical material pertinent to NASA's mission.

Specialized services also include creating custom thesauri, building customized databases, and organizing and publishing research results.

For more information about the NASA STI program, see the following:

Access the NASA STI program home page at *http://www.sti.nasa.gov.*

- E-mail your question via the Internet to help@sti.nasa.gov.

- Fax your question to the NASA STI Help Desk at (301) 621-0134.

- Phone the NASA STI Help Desk at (301) 621-0390.

- Write to:
  NASA STI Help Desk
  NASA Center for AeroSpace Information
  7121 Standard Drive
  Hanover, MD 21076-1320

NASA/TP-2006-213676

Extended Aging Theories for Predictions of Safe Operational Life of Critical Airborne Structural Components

William L. Ko and Tony Chen
NASA Dryden Flight Research Center
Edwards, California

National Aeronautics and
Space Administration

Dryden Flight Research Center
Edwards, California 93523-0273

May 2006

Cover art: NASA Dryden Flight Research Center, photograph number EC01-0182-20.

Available from the following:

NASA Center for AeroSpace Information
7121 Standard Drive
Hanover, MD 21076-1320
(301) 621-0390

National Technical Information Service
5285 Port Royal Road
Springfield, VA 22161-2171
(703) 605-6000

CONTENTS

ABSTRACT

The previously developed Ko closed-form aging theory has been reformulated into a more compact mathematical form for easier application. A new equivalent loading theory and empirical loading theories have also been developed and incorporated into the revised Ko aging theory for the prediction of a safe operational life of airborne failure-critical structural components. The new set of aging and loading theories were applied to predict the safe number of flights for the B-52B aircraft to carry a launch vehicle, the structural life of critical components consumed by load excursion to proof load value, and the ground-sitting life of B-52B pylon failure-critical structural components. A special life prediction method was developed for the preflight predictions of operational life of failure-critical structural components of the B-52H pylon system, for which no flight data are available.

NOMENCLATURE

A	crack location parameter (A = 1.12 for a surface crack)
a	depth of semi-elliptic surface crack, in.
a_c^o	operational limit crack size, in., $a_c^o = \frac{Q}{\pi}\left(\frac{K_{IC}}{AM_K f\sigma^*}\right)^2 = \frac{a_c^p}{f^2}$
a_c^p	initial crack size associated with proof (or limit) load, in., $a_c^p = \frac{Q}{\pi}\left(\frac{K_{IC}}{AM_K\sigma^*}\right)^2$
$(a_c^p)_{old}$	initial crack based on original proof load test, in.
$(a_c^p)_{new}$	initial crack based on revised proof load test, in.
a_1	crack size at the end of the first flight, in. $a_c^p + \Delta a_1$
C	coefficient of Walker crack growth equation, $\frac{\text{in.}}{\text{cycle}}\left(\text{ksi}\sqrt{\text{in.}}\right)^{-\text{m}}$
c	half-length of surface crack, in.
D	diameter
E	complete elliptic function of the second kind, $E = \int_0^{\pi/2} \sqrt{1-k^2\sin^2\phi}\,d\phi$
F_1^*	number of flights predicted from Ko closed-form aging theory
F_p	number of flights consumed by the proof load
f	operational load factor associated with the worst cycle of a random loading spectrum, $f = V_{\max}^o / V^*, (f < 1)$
$\bar{f}$	equivalent loading factor associated with an equivalent-constant-amplitude loading spectrum, $\bar{f} = V_{\max} / V^*, (\bar{f} < f)$
HF	B-52H front hook
HR	B-52H rear hook
HFF	B-52H front fitting

HRF	B-52H rear fitting
HLSB	B-52H pylon lower sway brace
HXLV	Hyper-X launch vehicle
i	1, 2, 3, …. , integer associated with the i-th half-cycle
K_{IC}	mode I critical stress intensity factor, ksi$\sqrt{\text{in.}}$
$K_{\max}$	mode I stress intensity factor associated with $\sigma_{\max}$, ksi$\sqrt{\text{in.}}$
ΔK	mode I stress intensity amplitude associated with stress amplitude, $(\sigma_{\max} - \sigma_{\min})$, ksi$\sqrt{\text{in.}}$
ksi	1000 times lb/in^2
k	modulus of elliptic function, $k = \sqrt{1-(a/c)^2}$
M_k	flaw magnification factor (M_k = 1 for a shallow crack)
m	Walker exponent associated with $K_{\max}$
N	number of stress cycles
N_1	number of stress cycles consumed during the first flight
n	Walker exponent associated with R
Q	surface flaw and plasticity factor, $Q = [E(k)]^2 - 0.212(\sigma^*/\sigma_Y)^2$
R	radius
R^o	stress or load ratio associated with the worst cycle of random loading spectrum, $R^o = \sigma^o_{\min} / \sigma^o_{\max} = V^o_{\min}/V^o_{\max}$
R	stress or load ratio associated with constant-amplitude loading spectrum, $R = \sigma_{\min} / \sigma_{\max} = V_{\min}/V_{\max}$
SRB/DTV	solid rocket booster/drop test vehicle
SUL	Pegasus pylon, left shackle upper part
SUR	Pegasus pylon, right shackle upper part
SLL	Pegasus pylon, left shackle lower part
SLR	Pegasus pylon, right shackle lower part
t	thickness, in.
V	hook load, lb

V_A	B-52B pylon front hook load, lb
V_{BL}	B-52B pylon left rear hook load. lb
V_{BR}	B-52B pylon right rear hook load, lb
V_{PFL}	Pegasus pylon front left hook load, lb
V_{PFR}	Pegasus pylon front right hook load, lb
V_{PRL}	Pegasus pylon rear left hook load, lb
V_{PRR}	Pegasus pylon rear right hook load, lb
VA	B-52B pylon front hook
VBL	B-52B pylon left rear hook
VBR	B-52B pylon right rear hook
VPFL	Pegasus pylon front left hook
VPFR	Pegasus pylon front right hook
VPRL	Pegasus pylon rear left hook
VPRR	Pegasus pylon rear right hook
V^*	proof load for any critical structural component, lb
V	applied load for any critical structural component, lb
$V^o_{\max}$	maximum load of the worst cycle of random loading spectrum, lb
$V^o_{\min}$	minimum load of the worst cycle of random loading spectrum, lb
$V_{\max}$	maximum load of equivalent constant amplitude loading spectrum, lb
$V_{\min}$	minimum load of equivalent constant amplitude loading spectrum, lb
V_S	mean load of equivalent constant amplitude loading spectrum, lb, $V_S = (1/2)(V_{\max} + V_{\min})$
W	weight of launch vehicle, lb
α	coefficient of thermal expansion
Δa_1	amount of crack growth induced by the first flight, in.
Δa_G	ground-sitting crack growth, in.
Δa_p	amount of crack growth induced by the proof load, in.
δa_i	crack growth induced by the *i*-th half cycle, in.

η stress-load coefficient, ksi/lb, $\eta = \sigma^* / V^*$

θ_c angular location of critical stress point, rad

ν Poisson ratio

ρ density, lb/in^3

σ^* tangential stress at critical stress point induced by the proof (limit) load V^*, ksi, $\sigma^* = \eta V^*$

σ_A tangential stress at critical stress point of B-52B pylon front hook induced by V_A, ksi

σ_{BL} tangential stress at critical stress point of B-52B pylon rear left hook induced by V_{BL}, ksi

σ_{BR} tangential stress at critical stress point of B-52B pylon rear right hook induced by V_{BR}, ksi

σ_{PFL} tangential stress at critical stress point of Pegasus pylon front left hook induced by V_{PFL}, ksi

σ_{PFR} tangential stress at critical stress point of Pegasus pylon front right hook induced by V_{PFR}, ksi

σ_{PRL} tangential stress at critical stress point of Pegasus pylon rear left hook induced by V_{PRL}, ksi

σ_{PRR} tangential stress at critical stress point of Pegasus pylon rear right hook induced by V_{PRR}, ksi

$\sigma^o_{\max}$ tangential stress at critical stress point associated with operational peak load, $V^o_{\max}$, ksi

σ_U ultimate tensile stress, ksi

σ_Y yield stress, ksi

$\sigma_{\max}$ maximum stress of constant amplitude loading cycles, ksi

$\sigma_{\min}$ minimum stress of constant amplitude loading cycles, ksi

σ_t tangential stress along hook inner boundary, ksi

$(\sigma_t)_{\max}$ maximum value of σ_t, ksi

σ_θ tangential stress in θ-direction, ksi

$(\sigma_\theta)_{\max}$ maximum value of σ_θ, ksi

τ_U	ultimate shear stress, ksi
ϕ	angular coordinate for semielliptic surface crack, rad
$( )_i$	quantity associated with the *i*-th half-cycle of random loading spectrum
$( )^*$	quantity associated with proof load

INTRODUCTION

Load-carrying structural components with L-shaped geometry or containing holes will certainly have stress concentration problems. When subjected to cyclic loading, the peak stress concentration point could be with fatigue crack initiation sites. The structural components, which contain stress concentration sites, may be called failure-critical structural components.

The NASA Dryden B-52B launch aircraft has been used to carry various types of flight research vehicles for high-altitude air-launching tests. The test vehicle is mated to the B-52B aircraft pylon through one L-shaped front hook and two identical L-shaped rear hooks. The L-shaped geometry always induces a stress concentration problem in the hooks. The critical stress point at the hook inner boundary, where the tangential tensile stress reaches a maximum at the inner curved boundary, is the potential fatigue crack initiation site.

During the early stages (1983) of the air-launching tests of the solid rocket booster drop test vehicle (SRB/DTV, 49,000 lb), the two B-52B pylon rear hooks (made of 4340 steel) failed almost simultaneously during the towing of the B-52B carrying the SRB/DTV on a relatively smooth taxiway (low-amplitude dynamic loading). Microscopic examinations of the hook fracture surfaces revealed that the left rear hook had a micro-surface crack of 0.031 in. deep, and the right rear hook had a 0.038-in. deep micro-surface crack at the respective critical stress points at each hook inner boundary (ref. 8). Those micro-surface cracks escaped preflight detection because of masking by the plating film. Those fatigue cracks must have been initiated from the past repeated cyclic loadings under different flight test programs, and possibly from surface corrosion. Fortunately, the hook failures occurred during taxiing. If the hook failures would have occurred during the takeoff run or during the captive flight, a catastrophic accident could have occurred. This type of accident underscores the need for development of reliable aging theories for accurate operational life predictions of failure-critical structural components of any air launching system (e.g., B-52B pylon, Pegasus® (Orbital Sciences Corporation, Dulles, Virginia) adapter pylon, and B-52H pylon).

Currently, the B-52B aircraft is to carry, through a special Pegasus adapter pylon, the Hyper-X launch vehicle (HXLV) air-launching of (40,000 lb) for the X-43 flight research vehicle (3,000 lb) for a Mach 7~10 hypersonic flight test. The Pegasus adapter pylon has several failure-critical components (two identical Pegasus adapter shackles with rectangular and circular holes, and four identical L-shaped Pegasus hooks). The operational life spans of those components are still not known.

Also, the newly acquired B-52H aircraft is to be used for air launching of the X-37 (7,000 lb) approach and landing test vehicle. The X-37 is to be carried by two identical L-shaped pylon hooks. The two B52-H pylon hooks and several B-52-H pylon structural components are all failure critical, and the operational life spans are yet to be determined.

The accuracy of the aging theory hinges upon accurate calculations of flight-induced crack growth at the critical stress point of a failure-critical structural component (e.g., B-52B hooks). In the past aging theories developed by Ko (refs. 1~5), the half-cycle theory (ref. 6) was applied to calculate the amount of crack growth in a failure critical component caused by flight random loading.

Recently, in order to account for the progressive nature of crack growth, the Walker crack-growth equation was applied, and the closed-form aging theory was developed by Ko (ref. 5) for predictions of a safe operational life span of failure-critical structural components when half-cycle computer programs are not available. The past Ko aging equation (ref. 5) was formulated in terms of crack sizes and needed to be reformulated into a more compact form for easier application.

In the present report, a new equivalent loading theory and empirical loading theories have been developed based on the past SRB/DTV flight data. The newly developed loading theories can then be combined with the revised Ko closed-form aging theory (ref. 5) for predictions of safe operational life spans of various airborne failure-critical structural components.

AIR-LAUNCHING CASES

In the operational life analysis, three air-lunching cases are considered, the B-52 B aircraft carrying the SRB/DTV, the B-52B carrying the HXLV/ X-43 system and the B-52H carrying the X-37 vehicle. A description of each case follows.

B-52B Aircraft Carrying the Solid Rocket Booster and Drop Test Vehicle (SRB/DTV)

Figure 1 shows the B-52B aircraft carrying the previously tested solid rocket booster drop test vehicle (SRB/DTV, 49,000 lb). The test vehicle is mated to the B-52B aircraft pylon through one front hook and two identical rear hooks, all of which are L-shaped, and therefore failure-critical. The operational life spans of B-52B pylon hooks carrying SRB/DTV have been well-established (refs. 1~5). The past SRB/DTV flight data is used to establish the equivalent loading theory and the empirical loading theories for predictions of operational life of failure-critical structural components for the following two air-launching cases.

The B-52B Aircraft Carrying the HXLV and X-43 Vehicle

Figure 2 shows the B-52B aircraft carrying the HXLV/X-43 system (40,000 lb) for flight tests of the X-43 hypersonic flight research vehicle (3,000 lb) up to Mach 7~10 (ref. 7). Because the Pegasus booster rocket has a delta wing that prevents the booster cylindrical body from nesting closely under the B-52B pylon concave belly, the Pegasus adapter pylon had to be used to carry the HXLV/X-43 system by four identical Pegasus pylon hooks. The Pegasus pylon itself is then carried by the B-52B pylon hooks using a double-shear pin that hangs on the B-52B front hook and through Pegasus pylon adapter shackles to hook on the B-52B two rear hooks. The failure-critical structural components identified are: The Pegasus pylon adapter shackles, which contain rectangular and circular holes, and the L-shaped Pegasus pylon hooks.

B-52H Aircraft Carrying the X-37 Vehicle.

Figure 3 shows the newly acquired B-52H aircraft that is to be used to carry the X-37 approach and landing test vehicle (7,000 lb) for air launching. The X-37 is to be carried by the B-52H pylon with two L-shaped hooks similar to those used to carry the X-38 (ref. 8). The B-52H pylon (fig. 3 inset) is attached to the B-52H wing using two front fittings and one rear fitting. The failure-critical structural components identified for the B-52H pylon structure are: the B-52H pylon L-shaped hooks, the B-52H pylon front and rear fittings with holes, and a B-52H pylon lower sway brace containing holes.

FAILURE-CRITICAL COMPONENTS

Appendix A describes the geometry and the stress distributions of the above air-launching systems failure-critical structural components (refs. 9~10). Namely, B-52B pylon hooks (figs. 4~7), Pegasus pylon adapter shackles (figs. 8~10), Pegasus pylon hooks (figs. 11~12), B-52H pylon hooks (figs. 13~14), a B-52H pylon front fitting (figs 15~16), a B-52H pylon rear fitting (figs. 17~18), and a B-52H pylon lower sway brace (figs. 19~20). The operational life of those failure-critical components is estimated using the revised Ko operational life theory and the empirical loading theories developed in the following sections from the past SRB/DTV flight data.

OPERATIONAL LIFE THEORY

In the following sections, a new equivalent loading theory and a special empirical loading theory are developed, and then incorporated into the original Ko closed-form aging theory (ref. 5) to predict the flight test operational life.

Operational Life Equation

To account for the progressive crack growth under a random loading spectrum, the Walker crack-growth rate equation was borrowed for the calculations of the amounts of crack growths for all successive flights (refs. 3, 4). Assuming that all flights have the same loading spectra and the same flight durations, Ko (ref. 5) developed the closed-form aging theory resulting in the following operational life equation for calculations of the maximum number of flights F_1^*.

$$F_1^* = \frac{(a_c^p)^{1-\frac{m}{2}} - (a_c^o)^{1-\frac{m}{2}}}{(a_c^p)^{1-\frac{m}{2}} - (a_1)^{1-\frac{m}{2}}} = \frac{1 - \left(\frac{a_c^p}{a_c^o}\right)^{\frac{m}{2}-1}}{1 - \left(\frac{a_c^p}{a_1}\right)^{\frac{m}{2}-1}} \tag{1}$$

In equation (1), m is the Walker stress-intensity-amplitude-exponent (refs. 3, 4), a_c^p is the initial fictitious crack size associated with the proof load, a_c^o is the operational crack size associated with the peak operational load, and a_1 is the crack size at the end of the first flight.

The initial and the operational crack sizes $\{a_c^p, a_c^o\}$ in equation (1) are to be calculated respectively from the following crack tip equations based on fracture mechanics (refs 1~4).

$$a_c^p = \frac{Q}{\pi}\left(\frac{K_{IC}}{AM_K\sigma^*}\right)^2 \tag{2}$$

$$a_c^o = \frac{Q}{\pi}\left(\frac{K_{IC}}{AM_K\sigma_{\max}^o}\right)^2 = \frac{a_c^p}{f^2}; f = \frac{\sigma_{\max}^o}{\sigma^*} < 1 \tag{3}$$

and the first flight-induced crack size, a_1 in equation (1), is given by

$$a_1 = a_c^p + \Delta a_1 \tag{4}$$

where Δa_1 is the amount of crack growth induced by the first flight. The calculations of the crack growth, Δa_1, is described in detail in reference 2.

In equations (2) and (3), K_{IC} is the Mode I critical stress intensity factor, A is the crack location parameter (for a surface crack, A = 1.12, refs. 1~4), M_k is the flaw magnification factor (for a shallow surface crack, M_k = 1.0, refs. 1~4), and finally, Q is the surface flaw shape and plasticity factor for an elliptic surface crack (surface length 2c, depth a) and is expressed as (refs. 1~4).

$$Q = \left[E(k)\right]^2 - 0.212\left(\frac{\sigma^*}{\sigma_Y}\right)^2; \; E(k) = \int_0^{\pi/2}\sqrt{1-k^2\sin^2\phi}\,d\phi \; ; \; k = \sqrt{1-\left(\frac{a}{c}\right)^2} \tag{5}$$

where σ_Y is the yield stress, and $E(k)$ is the complete elliptic function of the second kind defined, ϕ is the angular coordinate for a semi-elliptic surface crack (refs. 1~4), and k is the modulus of the elliptic function.

Also, in equations (2) and (3), $\{\sigma^*, \sigma_{\max}^o\}$ are the peak tangential tensile stresses at the critical stress point associated respectively with the proof load and the operation peak load $\{V^*, V_{\max}^o\}$; $f\,(< 1)$ is the operational load factor associated with the peak $\{\sigma_{\max}^o, V_{\max}^o\}$ of the random loading spectrum. Because $f < 1$, the size of a_c^o is naturally much larger than that of a_c^p .

The crack size differential $(a_c^o - a_c^p)$ then gives the available range that the cumulative crack growth can reach, and is the key factor for determining the number of safe operational flights.

In light of equation (3), the operational life equation (1) may be rewritten in the following more compact mathematical form.

$$F_1^* = \frac{1 - f^{m-2}}{1 - \left(1 + \dfrac{\Delta a_1}{a_c^p}\right)^{1-\frac{m}{2}}} \tag{6}$$

In equation (6), the material property m is known, the load factor f is determined from the loading spectrum of the first flight, and the initial crack size, a_c^p , is calculated from equation (2) based on the proof load and given material and crack geometrical properties. But, the crack growth Δa_1 remains to be determined. The accuracy of operational life prediction hinges upon accurate calculations of the crack growth, Δa_1. For accurate calculations of Δa_1, the half-cycle theory (ref. 6) was found to be the most accurate crack-growth theory used, because it picks up the damage (crack growth) induced by every half-cycle of the random loading spectrum without neglecting the infinitesimal half cycles which do not even cross the mean stress line (refs. 1, 2, 6).

Stress-Load Equation

In the actual flight tests, the applied loads (such as hook loads) on the critical structural components are usually measured by means of strain gages. In order to know the tensile stress level (e.g σ^*) at the critical stress point, the applied load (e.g V^*) must be related to the stress through the following stress-load relationship

$$\sigma^* = \eta V^* \tag{7}$$

where η is the stress-load coefficient, and can be determined from the finite-element stress analysis of the critical structural component (ref. 10). In light of equation (7), the load factor f [eq. (3)] may be rewritten as

$$f = \frac{\sigma_{\max}^o}{\sigma^*} = \frac{V_{\max}^o}{V^*}; f < 1 \tag{8}$$

Crack Growth Equations

The crack growth, Δa_1, induced by the random loading spectrum of the first flight [(eq. (4)] may be calculated using the half-cycle theory (refs. 1~5). The half-cycle theory assumes that the amount of crack growth, δa_i ,caused by the *i*-th (i = 1, 2, 3,…..) half-cycle of the random loading spectrum may be calculated from the Walker crack growth rate equation:

$$\frac{da}{dN} = C(K_{\max})^m(1-R)^n = C(\Delta K)^m(1-R)^{n-m} \tag{9}$$

by setting $da = \delta a_i$ and dN = 1/2. Namely,

$$\delta a_i = \frac{C}{2}\left[(K_{\max})_i\right]^m(1-R_i)^n = \frac{C}{2}(\Delta K_i)^m(1-R_i)^{n-m} \tag{10}$$

with

$$\left(K_{\max}\right)_i = AM_k\left(\sigma_{\max}\right)_i\sqrt{\frac{\pi a_{i-1}}{Q}} \tag{11}$$

$$(\Delta K)_i = AM_k\left[(\sigma_{\max})_i - (\sigma_{\min})_i\right]\sqrt{\frac{\pi a_{i-1}}{Q}} \tag{12}$$

$$R_i = \frac{(\sigma_{\min})_i}{(\sigma_{\max})_i} \tag{13}$$

where the subscript i (i = 1, 2, 3, ….) is associated with the *i*-th half-cycle, and a_{i-1} is the crack size at the end of the (i - 1)-th half-cycle.

If N_1 is the total number of random stress (or load) cycles induced by the first flight, then the amount of crack growth, Δa_1, induced by the first flight may be calculated from the following half-cycle crack growth equation

$$\Delta a_1 = \sum_{i=1}^{2N_1} \delta a_i \tag{14}$$

In equation (14), the calculation of the right-hand side can be carried out by means of special crack growth computer programs (developed during the SRB/DTV era). These programs read the entire random loading spectra and pick up the values $\{(\sigma_{\max})_i, (\sigma_{\min})_i\}$ of the *i*-th half-cycle, and calculate the crack growth increment, δa_i, from equation (10) for each half-cycle; and then sum up δa_i over $2N_1$ half-cycles (not N_1) to obtain the value of Δa_1. The graphical summing up

δa_i induced by the half-cycles of a random loading spectrum is illustrated in figures 3 and 4 of reference 2.

The predictions of fatigue life using the half-cycle theory compares fairly well with some limited number of experimental fatigue data reported in reference 6 (p. 211).

EQUIVALENT LOADING THEORY

During the SRB/DTV flight test era (1983-1985), special crack growth computer programs were developed for the calculation of crack growth, Δa_1**,** for the B-52B hooks, using the half-cycle crack growth equation (14). After the completion of the SRB/DTV program (refs. 1~2), several conversions of central computer systems took place. Unfortunately, the tapes of the crack growth computer programs were lost during these conversions. Thus, it is not possible to use the half-cycle crack growth equation (14) to calculate Δa_1 for other flight test programs.

Therefore, an equivalent loading theory has been developed for the operational life predictions of failure-critical structural components when the half-cycle crack growth computer program is not functional. The equivalent loading theory uses the equivalent constant-amplitude loading spectrum (ref. 5) to represent the actual random loading spectrum with an assumption that the former induces an amount of crack growth equal to the amount of crack growth, Δa_1, calculated from the half-cycle crack growth equation (14).

Equivalent Crack Growth Equations

In the Walker crack growth rate equation (9), if da is replaced with crack growth Δa_1 induced by the first flight, and dN is replaced with N_1 (the number of load cycles consumed during the first flight), then equation (9) may be modified to express the amount of crack growth, Δa_1, as

$$\Delta a_1 = C\left(AM_k \sigma_{\max} \sqrt{\frac{\pi a_c^p}{Q}} \right)^m (1-R)^n N_1 \tag{15}$$

which, in light of stress-load equation (7), becomes

$$\Delta a_1 = C\left(AM_k \bar{f} \eta V^* \sqrt{\frac{\pi a_c^p}{Q}} \right)^m (1-R)^n N_1 \tag{16}$$

where $\bar{f}$ is the load factor associated with the equivalent constant amplitude loading spectrum, and which is defined as [see eq. (8)],

$$\bar{f} = \frac{\sigma_{\max}}{\sigma^*} = \frac{V_{\max}}{V^*} \ ; \ \sigma_{\max} = \eta V_{ma} \tag{17}$$

where $\{\sigma_{max}, V_{max}\}$ are respectively the maximum stress and maximum load of the equivalent constant amplitude loading spectrum. Keep in mind that the value of $\bar{f}$ is always smaller than the load factor f ($f > \bar{f}$) associated with the actual random loading spectrum.

Equivalent Loading Spectrum

Figure 21 illustrates the random loading spectrum represented with an equivalent constant amplitude loading spectrum assuming that both loading spectra induce identical crack growth, Δa_1. Because the crack growth, Δa_1, expressed by equation (16) is set equal to the crack growth, Δa_1, calculated from the half-cycle crack growth equation (14) (like the SRB/DTV case), equation (16) may be rearranged, in light of equation (17), as

$$(\bar{f})^m (1-R)^n = \underbrace{\frac{\Delta a_1}{CN_1}\left(\frac{1}{AM_k \eta V^*}\sqrt{\frac{Q}{\pi a_c^p}}\right)^m}_{\text{|<-------------known------------->|}} \tag{18}$$

Equation (18) is for determining the loading intensity of the equivalent constant-amplitude loading spectrum. The right-hand side of equation (18) is known, but the left-hand side has two unknowns $\{\bar{f}, R\}$ to be determined in order to establish the equivalent constant-amplitude loading spectrum. In fact, equation (18) is not an ideal form for solving for the two unknowns $\{\bar{f}, R\}$ because it is hard to pick the value of R and solve for $\bar{f}$ or vice versa. It is more practical to solve equation (18) in terms of loads as described below. The stress (or load) ratio, R, may be expressed as

$$R = \frac{\sigma_{min}}{\sigma_{max}} = \frac{V_{min}}{V_{max}} = 2\frac{V_S}{V_{max}} - 1 \tag{19}$$

where $\{V_{min}, V_S\}$ are respectively the minimum load and the mean load of the equivalent constant-amplitude loading spectrum. In light of equation (19), equation (18) may be written in terms of loads as

$$(V_{max})^m \left(1 - \frac{V_S}{V_{max}}\right)^n = \underbrace{\frac{\Delta a_1}{2^n CN_1}\left(\frac{1}{AM_k \eta}\sqrt{\frac{Q}{\pi a_c^p}}\right)^m}_{\text{|<-------------known------------->|}} \tag{20}$$

Because equation (20) has two unknown loads $\{V_{max}, V_S\}$ on the left-hand side, there are multiple sets of $\{V_{max}, V_S\}$ which satisfy equation (20). This implies that there are multiple equivalent constant amplitude load spectra, all of which induce the same amount of crack growth, Δa_1. One practical approach is to choose the value of the mean load, V_S, and solve for the second unknown maximum load V_{max} from equation (20). Thus, the equivalent constant-amplitude load spectrum could be established. Based on the values of $\{V_{max}, V_S\}$ thus determined, the values of $\{\bar{f}, R\}$ may then be calculated from equations (17) and (19) respectively.

In establishing the equivalent constant-amplitude loading spectrum, one option is to choose the mean load V_S of the equivalent constant-amplitude load spectrum to match the mean load of the worst cycle of the actual random loading spectrum (fig. 21). Namely,

$$V_S = \frac{1}{2}(V_{\max} + V_{\min}) = \frac{1}{2}(V^o_{\max} + V^o_{\min}) \tag{21}$$

where $\{V^o_{\max}, V^o_{\min}\}$ are respectively the maximum and minimum loads of the worst cycle of the random loading spectrum. Using the relationships $f = V^o_{\max} / V^*$ [eq. (8)] and the definition of the stress (or load) ratio R^o

$$R^o = \frac{\sigma^o_{\min}}{\sigma^o_{\max}} = \frac{V^o_{\min}}{V^o_{\max}} \tag{22}$$

equation (21) takes on the form.

$$(1+R)\bar{f} = (1+R^o)f \tag{23}$$

which functionally relates $\{\bar{f}, R\}$ to $\{f, R^o\}$ of the actual random load spectrum.

The equivalent crack growth theory described above is a powerful alternative crack growth theory for calculating crack growth, Δa_1, from equation (16) based on $\{\bar{f}, R\}$ values in case the half-cycle crack growth equation (14) cannot be used.

THE SRB/DTV CASE

A table of stress-load coefficients and a description of crack geometry follow. Flight data, both original and revised, are also provided.

Stress-Load Coefficients

Through finite-element stress analysis (ref. 10), the original stress-load coefficients (η) for stress-load equations $\sigma^* = \eta\, V^*$ [eq. (7)] of the B-52B hooks are listed in table 1 (refs. 1 and 2).

Table 1. Stress-load coefficients, η, for B-52B hooks established from finite-element stress analysis (ref. 10).

Critical structural components	Stess - Load Coefficient, η, ksi/lb
B-52B front hook (VA)	7.3522×10^{-3}
B-52B left rear hook (VBL)	5.8442×10^{-3}
B-52B right rear hook (VBR)	5.8442×10^{-3}

Crack Geometry Description

In calculations of the initial crack, a_c^p [eq. (2) for the B-52B hooks], and crack growth, Δa_1 [eq. (14) or (16)], the surface crack (A = 1.12) is assumed to be very shallow (i.e., M_k = 1), and is a semi-elliptic crack with aspect ratio a/2c = 1/4. This is the aspect ratio of the surface crack observed in one of the failed B-52B rear hooks made of 4340 steel (1983), designated "old." (ref. 8). For the crack aspect ratio $a/2c$ = 1/4, and using the peak stress ratio $\sigma^* / \sigma_Y = 1$, equation (5) gives the value of Q as $Q = (1.2111)^2 - 0.212 \times 1$ = 1.2548. Finally, the values of K_{IC} and other material properties used in the numerical calculations are listed in appendix-b.

Original SRB/DTV Flight Data

The original flight data of B-52B hooks carrying SRB/DTV (figs 1, 4~7) taken from reference 1 are listed in table 2. The original random loading spectra had 4Hz frequencies, and the average flight time was 50 min. (i.e., N_1= 50 × 60 × 4 = 12,000 cycles per flight).

Table 2. Original data of B-52B pylon hooks carrying SRB/DTV (49.000 lb); SRB/DTV proof loads; 50 min./flight; 4 Hz (ref. 1)

B-52B hooks	V^*, lb	η, ksi/lb	a_c^p, in.	f	R^o	Δa_1, in.	F_1^*, flights
Front hook (VA)	36,520	7.3522-3	0.0990	0.5479	0.5000	1.8295-3	42†
Left rear hook (VBL)	44,110	5.8442-3	0.0734	0.4583	0.8113	0.5887-3	125
Right rear hook (VBR)	44,230	5.8442-3	0.0730	0.4497	0.7885	0.7705-3	96

† Shortest operational life.

In table 2, the values of $\{f, R^o\}$ are associated with the worst loading cycle (maximum f and maximum R^o) during taxiing (fig. 5, ref. 5)]; a_c^p were calculated from equation (2) using the original proof loads shown in table 1; with the crack growths, Δa_1, calculated using the half-cycle crack growth equation (14); and the number of flights, F_1^*, were calculated from equation (6).

Revised SRB/DTV Flight Data

To match the proof loads $\{V_A^* = 36{,}500$ lb, $V_{BL}^* = V_{BR}^* = 57{,}819$ lb$\}$ used in the HXLV/X-43 case, table 2 must be revised. Using the same set of input data mentioned above, the new initial crack sizes, a_c^p, were recalculated from equation (2), and in light of equation (15), the new crack growths, Δa_1, were calculated from

$$(\Delta a_1)_{new} = \left[\frac{(a_c^p)_{new}}{(a_c^p)_{old}}\right]^{\frac{m}{2}} (\Delta a_1)_{old} \tag{24}$$

where $(a_c^p)_{old}$, $(a_c^p)_{new}$ are the initial cracks associated, respectively, with the original proof loads for the SRB/DTV case 1983 (table 2) and the new proof loads for the HXLV/X43 case. The resulting new set of data is listed in Table 3.

Table 3. Revised data for B-52B pylon hooks carrying SRB/DTV (49,000 lb) using HXLV/ X-43 proof loads; 50 min./flight; 4 Hz.

B-52B hooks	V^*, lb	η, ksi/lb	a_c^p, in.	f	R^o	Δa_1, in.	F_1^*, flights
Front hook (VA)	36,520	7.3522-3	0.0691	0.5479	0.5000	0.9512-3	57*
Left rear hook (VBL)	57,819	5.8442-3	0.0429	0.4583	0.8113	0.2451-3	176
Right rear hook (VBR)	57,819	5.8442-3	0.0429	0.4497	0.7885	0.3236-3	135

In table 3, the numbers of flights, F_1^*, were calculated from equation (6) using the data shown in table 3. The values of $\{f, R^o\}$ listed in Table 3 are used to develop the empirical loading theories for the case of B-52B carrying HXLV/X-43 and other cases.

EMPIRICAL LOADING THEORY

The purpose of the empirical loading theory is to determine the values of the equivalent load factor and load ratio $\{\bar{f}, R\}$ associated with the equivalent constant-amplitude loading spectrum for the calculations of the crack growth, Δa_1, using equivalent crack growth equation (16).

The new empirical loading theory is developed based on the revised SRB/DTV flight data presented in table 3. The new empirical loading theory could be very useful in operational analysis of the following two cases. In one case when the actual flight data are available, but the crack growth, Δa_1, must be calculated from the equivalent crack growth equation (16) (such as the HXLV/X-43 case); or another case when the actual flight loading spectra are not yet available (such as the X-37 case).

Determinations of Both Load Factor and Stress (Load) Ratio Associated with the Constant-Amplitude Loading Factor

Based on the data presented in table 3, the unknown values of $\bar{f}$ and R for the equivalent constant amplitude loading spectra for the SRB/DTV case were calculated using the method described in the section, called "Equivalent Loading Theory". Thus, the equivalent constant amplitude loading spectra could be established. The values of $\bar{f}$ and R calculated from equations (17) and (19) after solving equation (20) for three B-52B pylon hooks carrying SRB/DTV are listed in table 4 together with the known values of f and R^o and the HXLV/X-43 proof load for the B-52B pylon hooks (figs. 4, and 6).

Table 4. Load data for B-52B hooks carrying SRB/DTV (49.000 lb).

B-52B hooks	V^*, lb	f	R^o	$\bar{f}$	R
Front hook (VA)	36,500	0.5479	0.5000	0.4295	0.9137
Left rear hook (VBL)	57,819	0.4583	0.8113	0.4202	0.9755
Right rear hook (VBR)	57,819	0.4497	0.7885	0.4083	0.9696

Load-Factor Equations

Figure 22 shows the calculated values of $\bar{f}$ plotted as functions of known values of f for the B-52B hooks carrying SRB/DTV (Table 3). For each of the B-52B hooks, $\bar{f}$ may be expressed as a linear function of f (load-factor equations).

B-52B front hook (VA):

$$\bar{f} = 0.7839 f \tag{25}$$

B-52B rear hooks (VBL, VBR):

$$\bar{f} = 0.9124 f \tag{26}$$

Load-Ratio Equations

Figure 23 shows $(1 - R)$ plotted as a function of $(1 - R^o)$ based on the SRB/DTV flight data listed in table 3. The relationships between $(1 - R)$ and $(1 - R^o)$ for the B-52B pylon hooks may be expressed with the following linear function (load-ratio equation).

B-52B front hook (VA):

$$\frac{1-R}{1-R^{o}} = 0.1726 \quad \text{or} \quad R = 0.8274 + 0.1726R^{o} \tag{27}$$

B-52B rear hooks (VBL, VBR):

$$\frac{1-R}{1-R^{o}} = 0.1368 \quad \text{or} \quad R = 0.8632 + 0.1368R^{o} \tag{28}$$

As is discussed in the following HXLV/X-43 case, the above load-factor equations (25) and (26), and the load-ratio equations (27) and (28) may be used as powerful tools for the calculation of the operational life spans of the B-52B hooks carrying the HXLV/X-43 system.

APPLICATION TO THE HXLV/X-43 CASE

The empirical equations presented in the previous section are now applied to the calculations of the operational life of B-52B hooks carrying the HXLV/X-43 system (figure 2). Figures 24 ~ 26 respectively show the loading spectra of B-52B hooks carrying the HXLV/X-43 during taxiing. The average flight duration for the HXLV/X-43 case is 90 min. with an average loading frequency of 3 Hz (i.e., $N_1 = 90 \times 60 \times 3 = 16{,}200$ cycles per flight).

Because the original crack growth computer program is out of commission, the half-cycle crack growth equation (14) cannot be used to calculate Δa_1 for the HXLV/X-43 case. Therefore, the equivalent loading theory described above must be used. The values f and R^{o} can be determined from the worst cycle of actual taxiing loading spectra (figs. 24~26), but the values of $\bar{f}$ and R for the equivalent constant amplitude loading spectra are unknown. Therefore, the empirical equations (25)~(28) established from the SRB/DTV flight data may be applied to calculate the values of $\bar{f}$ and R for the calculations of the equivalent crack growth, Δa_1, from equation (16) for the HXLV/X43 case. The resulting key data established for B-52B hooks carrying the HXLV/X-43 are listed in table 5.

Table 5. Key data for B-52B hooks carrying the HXLV/X43 (40,000 lb); 90 min./flight; 3 Hz.

B-52B hooks	V^*, lb	η, ksi/lb	a_c^p, in.	f	R^o	$\bar{f}$	R	Δa_1, in.	F_1^*, flights
(VA)	36,500	7.3522-3	0.0691	0.4656	0.6111	0.3650†	0.9329†	0.4128-3	148
(VBL)	57,819	5.8442-3	0.0429	0.3720	0.8158	0.3394†	0.9748†	0.1735-3	283
(VBR)	57,819	5.8442-3	0.0429	0.3328	0.8235	0.3036†	0.9759†	0.1121-3	460

† Calculated from SRB/DTV empirical formulae (24)~(27).

Table 5 shows, the initial cracks, a_c^p, are taken from table 3, and the numbers of flights, F_1^*, were calculated from equation (6) using the data provided in table 5. The key numerical input values used are the same as the SRB/DTV case. Note that the number of flights, F_1^*, for the HXLV/X43 case in table 5 are much higher than the SRB/DTV case in table 3 because of a lighter store weight.

ADDITIONAL EMPIRICAL EQUATIONS

This section presents additional empirical formulae developed for the purpose of preflight operational life analysis of B-52B hooks carrying different store weight, *W,* when the actual loading spectra are not yet available. Based on both SRB/DTV and HXLV/X-43 flight data presented above, the weight-related empirical equations may be established for the B-52B hooks. It is assumed that the center of gravity of the new store is located in the vicinity of the center of gravity of SRB/DTV.

Load-Factor and Weight Relationship

Figure 27 shows the load factors, *f,* plotted as functions of the store weight, *W,* (lb) using both the SRB/DTV and HXLV/X43 flight data. The load factor, *f,* for each hook can be expressed as a linear function of the store weight, *W,* (lb) (load-factor/weight equations) as

B-52B front hook (VA)

$$f = 1.1411 \times 10^{-5} W \tag{29}$$

B-52B rear hooks (VBL, VBR)

$$f = 0.9265 \times 10^{-5} W \tag{30}$$

The above load-factor/weight equations are very useful in estimating the load factor, *f,* associated with different store weights, *W,* for conducting preflight operational life analysis.

Load-Ratio and Weight Relationship

Figure 28 shows the values of $(1-R^o)$ plotted as functions of the store weight, *W,* (lb) based on the flight data of B-52B hooks carrying SRB/DTV and B-52B hooks carrying the HXLV/X43 system. The value of $(1-R^o)$ for each B-52B hook may be expressed as a linear function of the store weight, *W,* (load-ratio/weight equations) as

B-52B front Hook (VA)

$$(1-R^o) = 1.0000W \times 10^{-5} \tag{31}$$

B-52B rear Hooks (VBL, VBR)

$$(1-R^o) = 0.4444W \times 10^{-5} \tag{32}$$

For the preflight operational life analysis when the actual loading spectrum is not yet available, the crack growth, Δa_1, may be calculated using the following empirical approach. When the new store weight, W, is given, the values of f and R^o may be found from figures 26 and 27, or calculated from equations (29)~(32). Once the values of f and R^o are determined, the unknown values of $\bar{f}$ and R for the equivalent constant amplitude loading spectra may be determined respectively from figures 22 and 23, or calculated from equations (25)~(27). Then, the crack growth, Δa_1, may be calculated from equation (16), and finally the number of flights, F_i^*, for each of the B-52B hooks may be calculated from the operational life equation (6). The empirical equations established above could also be applied to the operational life predictions of the following additional failure-critical structural components.

OPERATIONAL LIFE CALCULATIONS FOR FAILURE-CRITICAL COMPONENTS

Using the equivalent loading theory and the empirical loading theories described earlier, the safe operational numbers of flights, F_1^*, for each of the failure-critical structural components of the B-52B pylon, the Pegasus pylon, and B-52H pylon, were calculated using the revised Ko operational life equation. The detailed calculations are presented in Appendix C. In the calculations, the initial cracks, a_c^p, were calculated from equation (2) in light of equation (7) using the proper material properties (Appendix B), the associated proof loads, and the stress-load coefficients η (table C-1).

For the Pegasus pylon hooks, the load data f and R^o were determined from the worst cycle of the actual loading spectra during taxiing of the HXLV/X43 captive flight (figs. 22~32). The SRB/DTV empirical equations (26) and (28) were then used to calculate the values of $\bar{f}$ and R for the equivalent constant amplitude spectra representing the actual random loading spectra (figs. 22~32).

Tables 6 and 7 summarize the number of operational flights, F_1^*, for all the failure structural components considered taken from tables 3, 4, C-10, and C-11.

Table 6. Safe operational flights, F_1^*, for B-52B pylon components carrying SRB/DTV (49,000 lb, 50 min./flight) or HXLV/X-43 (40,000 lb, 90 min./flight).

B-52B pylon parts	F_1^* (HXLV/X-43), flights	F_1^* (SRB/DTV), flights
Front hook (VA)	148†	57†
Left rear hook (VBL)	283	176
Right rear hook (VBR)	460	135

Pegasus pylon	F_1^* (HXLV/X-43), flights
Shackle upper part left (SUL)	69‡ (414)§
Shackle upper part right (SUR)	108 (675)§
Shackle lower part left (SLL)	229
Shackle lower part left (SLR)	360
Front left hook (VPFL)	658
Front right hook (VPFR)	504
Rear left hook (VPRL)	2,292
Rear right hook (VPRR)	1,827

† Shortest operational life for B-52B hooks.

‡ Shortest operational life for Pegasus pylon components.

§ If AMAX is used.

Table 7. Safe operational flights, F_1^*, for B-52H pylon components carrying X-37 (7000 lb) approach/landing vehicle; 50 min./flight; 4Hz.

B-52H pylon parts	F_1^*, flights	
	Based on X-38 taxiing	Based on X-38 landing
Front hook (HF)	2,381†	1,079‡
Rear hook (HF)	4,820	485
Front fitting (HFF)	4,820	485
Rear fitting (HRF)	4,820	485
Lower sway brace (HLSB)	4,820	485

† Shortest life for taxiing case.

‡ Longest life landing case.

Keep in mind that the operational life spans presented in table 7 are the preflight-estimated values and are subject to updating once the actual flight loading spectra are available.

PROOF LOAD INDUCED STRUCTURAL LIFE CONSUMPTION

In this section, the number of flights the proof load spike consumes are examined. After the initial crack size, a_c^p , has been established based on the proof load, let us estimate the amount of crack growth, Δa_p, caused by a load excursion to the proof load value. For one spike of proof load, we have $\left[\bar{f} = 1, R = 0 \; (\sigma_{\min} = 0, \sigma_{\max} = \sigma^*), N = 1 \right]$, then equation (16) may be modified to express Δa_p as

$$\Delta a_p = C\left(AM_k(1)\eta V^* \sqrt{\frac{\pi a_c^p}{Q}} \right)^m (1-0)^n (1) = C\left(AM_k \eta V^* \sqrt{\frac{\pi a_c^p}{Q}} \right)^m \tag{33}$$

Since Δa_1 is the amount of crack growth per flight (first flight), the number of flights, F_p, consumed by one cycle of proof load (or limit load) may be obtained by dividing Δa_p by Δa_1 as

$$F_p = \frac{\Delta a_p}{\Delta a_1} = \frac{C}{\Delta a_1}\left(AM_k \eta V^* \sqrt{\frac{\pi a_c^p}{Q}} \right)^m \tag{34}$$

for which equation (33) was used.

In equation (34), Δa_1 may be calculated from equation (14) if the actual random loading data is available, or estimated from equation (16) for the preflight case when flight data is not yet available.

In light of equation (14) [or (16)], and using proper material properties given in Appendix B, the proof load consumed flights, F_p, were calculated from equation (34) for each critical component. The results are summarized in table 8 including the calculated values of Δa_1 and Δa_p.

Table 8. Number of flights consumed by one cycle of proof load.

Structural component	V^*, lb	Δa_1, in.	Δa_p,in.	$F_p\left(=\dfrac{\Delta a_p}{\Delta a_1}\right)$,flights
B-52B pylon front hook (VA)	36,500	0.4128-3	0.3264-3	0.7909
B-52B pylon left rear hooks (VBL)	57,819	0.1735-3	0.1786-3	1.0294
B-52B pylon right rear hooks (VBR)	57,819	0.1121-3	0.1786-3	1.5932
Pegasus pylon shackle upper left (SUL)	57,819	1.1490-3	0.3235-3	0.2816‡
Pegasus pylon shackle upper right (SUR)	57,819	0.7753-3	0.3235-3	0.4173
Pegasus pylon shackle lower left (SLL)	57,819	1.1491-3	0.3236-3	0.2816‡
Pegasus pylon shackle lower right (SLR)	57,819	0.7754-3	0.3236-3	0.4173
Pegasus pylon front left hook (VPFL)	75,000	0.2213-3	0.1785-3	0.8066
Pegasus pylon front right hook (VPFR)	75,000	0.2991-3	0.1785-3	0.5968
Pegasus pylon rear left hook (VPRL)	75,000	0.0830-3	0.1785-3	2.1506†
Pegasus pylon rear right hook (VPRR)	75,000	0.1001-3	0.1785-3	1.7832
B-52H pylon hook (HF)	123,198	0.3844-3	0.3234-3	0.8413
B-52H pylon hook (HR)	123,198	0.3844-3	0.3234-3	0.8413
B-52H pylon front fitting (HFF)	135,600	0.3844-3	0.3234-3	0.8413
B-52H pylon rear fitting (HRF)	34,791	0.3844-3	0.3234-3	0.8413
B-52H pylon lower sway brace (HLSB)	21,004	0.3844-3	0.3234-3	0.8413

† Highest Value.

‡ Lowest Value.

In table 16 the Pegasus pylon left shackle upper part has the lowest proof load consumed flights, 0.2815 flights; and the Pegasus pylon rear left hook has the highest proof load consumed flights, 2.1506 flights.

GROUND-SITTING LIFE

At the time of writing this report, the B-52B carrying the HXLV/X-43 had to stay on the ground for a number of days before taking off for an air-launching test. The ground-sitting loading is induced mostly by the wind, and has very low amplitude cycling in the vicinity of the static load. It is of vital importance to find out the crack growth induced by the ground sitting, and thereby to determine the maximum days allowable. Because the ground-sitting load spectra were obtained from an earlier captive flight, it is possible to estimate the ground-sitting life of the B-52B carrying the HXLV/X-43.

As presented in the operational life analysis of additional components, the Pegasus pylon left shackle upper part has the shortest operational life of 69 flights (table 6). The critical ground-sitting life component for the B-52B carrying the HXLV/X-43 is then the Pegasus pylon left shackle upper part.

Let $\{V_S,\ R^o\}$ respectively be the mean load and the stress ratio of a typical ground-sitting loading spectrum associated with the Pegasus shackle carrying the HXLV/X-43 vehicle, then the peak ground-sitting load $V_{\max}^o$ may be calculated from

$$V_{\max}^o = \frac{2}{1+R^o} V_S \tag{35}$$

In light of equation (8), the fractional load factor, f, may be calculated from

$$f = \frac{V_{\max}^o}{V^*} = \frac{2}{1+R^o} \frac{V_S}{V^*} \tag{36}$$

In equation (34), the proof load V^* for the Pegasus pylon shackle is $V^* = 57{,}819$ lb (table 5), and the ground-sitting mean load, V_S, and the stress ratio, R^o, were determined from the ground-sitting loading spectrum as

$$V_S = 19{,}400 \text{ lb} \tag{37}$$

$$R^o = 0.98 \sim 0.99 \tag{38}$$

The equivalent load factor, $\bar{f}$, and the equivalent stress ratio, *R,* associated with the equivalent constant-amplitude loading spectrum may be calculated respectively from equations (26) and (28) (associated with B-52B rear hooks). The key input loading data for the ground sitting the of B-52B carrying the HXLV/X-43 are listed in table 9.

Table 9. Ground-sitting input loading data for the B-52B carrying the HXLV/X-43.

R^o	f	$R\left(= 0.8632 + 0.1368 R^o\right)$	$\bar{f}\,(= 0.9124 f)$
0.980	0.3389	0.9973	0.3092
0.985	0.3381	0.9979	0.3085
0.990	0.3372	0.9986	0.3078

Let Δa_G be the ground-sitting crack growth induced by the ground-sitting random loading of N_1 cycles (cycles for one flight), then the equivalent crack growth equation (16) may be used to calculate the ground-sitting crack growth, Δa_G. The ground-sitting life, *GSL,* may then be calculated from the following equation

$$GSL = \frac{\Delta a_1}{\Delta a_G} F_1^* \times \frac{90}{60 \times 24} \text{days} \tag{39}$$

where $\Delta a_1 = 1.1490 \times 10^{-3}$ and $F_1^* = 69$ flights for the Pegasus pylon left shackle upper part.

The ground sitting life of the Pegasus pylon left shackle upper part, which determines the ground-sitting life of the B-52B carrying the HXLV/X-43, were calculated for different loading cases and are listed in table 10.

Table 10. Ground-sitting life of Pegasus pylon left shackle upper part (= Ground sitting life of the B-52B carrying the HXLV/X-43 $V^* = 57{,}816$ lb; $V_S = 19{,}400$ lb; $\Delta a_1 = 1.1490 \times 10^{-3}$ in.

R	$\bar{f}$	Δa_1, in.	Δa_G, in	*GSL*, day
0.980	0.3092	1.1490×10^{-3}	0.0365×10^{-3}	136
0.985	0.3085	1.1490×10^{-3}	0.0176×10^{-3}	282
0.990	0.3072	1.1490×10^{-3}	0.0143×10^{-3}	347

Table 10 shows that the ground-sitting life of B-52B carrying the HXLV/X-43 turned out to be quite long.

CONCLUDING REMARKS

Several theories have been developed for predictions of the operational life of airborne failure-critical structural components with the aid of earlier flight data. Highlights of these theoretical developments are summarized below.

1. The previously developed Ko closed-form aging theory has been reformulated into a more compact mathematical form for easier application.

2. A new equivalent loading theory and empirical loading theories have been developed and incorporated into the revised Ko aging theory for predictions of the safe operational life of airborne failure-critical structural components.

3. A new set of aging and loading theories have been applied to predict the safe number of air-launching flights, structural life consumed by load excursion to proof load value, and the ground-sitting life of the B-52B pylon failure-critical structural components.

4. A special operational life prediction method has been developed for estimations of the preflight operational life of failure-critical structural components of the B-52H pylon system, for which no flight data are available.

5. These operational life prediction theories developed here can be extended to any failure-critical structural components.

Dryden Flight Research Center
National Aeronautics and Space Administration,
Edwards, California, June 15, 2005

APPENDIX A
DESCRIPTIONS OF FAILURE-CRITICAL COMPONENTS

Appendix A briefly describes the failure-critical structural components of the B-52B pylon, the Pegasus adapter pylon, and the B-52H pylon for operational life analysis.

B-52B Pylon Hooks

Figure 4 shows the geometry of the B-52B front hook made of Inconel® 718 alloy*, and figure 5 shows the distribution of tangential stress along the inner boundary of the B-52B front hook with the stress-load equation shown (ref. 9). The critical stress point is defined as the point of $(\sigma_t)_{max}$.

Figure 6 shows the geometry of the B-52B rear hook made of AMAX MP-35N® alloy†, and figure 7 shows the distribution of tangential stress along the inner boundary of the B-52B rear hook with the stress-load equation shown (ref. 9). The critical stress point is at the point of $(\sigma_t)_{max}$.

Pegasus Pylon Adapter Shackle

As shown in figure 2, the Pegasus pylon is carried by the B-52 pylon through a double-shear pin mating the B-52B pylon front hook, and through two Pegasus pylon adapter shackles (simply "Pegasus shackle") connecting to the B-52B pylon two rear hooks. The geometry of a typical Pegasus pylon adapter shackle is shown in figure 8. The Pegasus shackles are made of PH13-8Mo® stainless steel‡. The double shear pin (not shown) is not fatigue critical because there is no critical stress point. However, the two Pegasus shackles (thickness 0.812 in.) are failure critical because each upper part has a rectangular hole (1.438 in. × 1.514 in.) with four rounded corners and a small radius of curvature of 0.093 in. (the inner boundary of B-52B rear hook (left or right) has a 0.5 in. radius of curvature). The Pegasus shackle lower part contains a circular pinhole of 1.25 in. diameter. Thus, the Pegasus shackle upper and lower regions have stress concentration problems, and so are failure critical.

The distribution of tangential stress along the inner boundary of the Pegasus pylon shackle upper part is shown in figure 9 with stress-load equations indicated (ref. 10). The distribution of tangential stress along the hole of the Pegasus shackle lower part is shown in figure 10 with stress load equations indicated (ref. 10).

---

* Inconel 718 is a registered trademark of Huntington Alloy Products Division, Internation Nickel Company, West Virginia.
† AMAX MP-35N is a trademark of SPS Technologies, Inc., Jenkinton, Pennsylvania.
‡ PH13-8Mo is a trademark of ARMCO Steel Corporation, Middletown, Ohio.

Pegasus Pylon Hooks

The Pegasus pylon (fig. 2) has four identical hooks made of AMAX MP-35N alloy (the same material used for B-52B pylon two rear hooks). Geometry of a typical Pegasus hook is shown in figure 11. This hook has a thickness of $t = 2$ in., and an inner radius of 0.51 in. The outer curved boundary has a 3.48-in. radius of curvature centered at different locations. The distribution of tangential stress along the inner boundary is shown in figure 12 with stress-load equations indicated (ref. 10).

B-52H Pylon Hook

Figure 13 shows the dimensions of the typical B-52H pylon hook, which is made of PH13-8Mo stainless steel. The B-52H hook, which has a shape very similar to that of X-38 hooks (ref. 7), is t =2.8-in. thick with an inner boundary radius of curvature of 0.5 in. (identical to that of the B-52B rear hook whose thickness is $t = 1.1$ in.). The distribution of tangential stress along the inner boundary of the hook is shown in figure 14 with the stress-load equation and critical stress point indicated (ref. 10).

B-52H Pylon Front Fitting

Figure 15 shows the geometry of the B-52H pylon typical front fitting, which is fabricated with PH13-8Mo stainless steel. The upper vertical triangular flange is $t = 1.125$-in. thick, with a circular hole containing a 1.379-in. radius, and the upper arc boundary having a 2.390-in. radius. The triangular region has a base angle of approximately 42.63 degrees. The distribution of tangential stress along the pinhole boundary is shown in figure 16 with stress-load equation and critical stress point indicated (ref. 10).

B-52H Pylon Rear Fitting

Figure 17 shows the geometry of the B-52H pylon rear fitting, which is fabricated with PH13-8Mo stainless steel. The rear fitting has two identical lugs, each of which has a thickness of $t = 0.39$ in. and a circular hole with a 1.495-in. radius, and a curved outer boundary with a 1.55-in. radius. The rest of key dimensions are indicated in figure 17. The distribution of tangential stress along the pinhole boundary is shown in figure 18 with stress-load equation and critical stress point indicated (ref. 10).

B-52H Pylon Lower Sway Brace

Figure 19 shows the geometry of the B-52H pylon lower sway brace, which is fabricated with PH13-8Mo stainless steel. The lower brace has four identical lugs, each of which has a thickness of $t = 0.50$ in. and a circular hole with a 1.00-in. diameter, with curved a boundary having a 1.00-in. radius. Other dimensions are indicated in figure 26. The distribution of tangential stress along the pinhole boundary is shown in figure 20 with stress-load equation and critical stress point indicated (ref. 10).

APPENDIX B
MATERIAL PROPERTIES

Material properties of the B-52B pylon, the Pegasus adapter pylon, and the B-52H pylon critical structural components are listed in Tables B-1 and B-2.

Table B-1. Material properties of critical structural components of the B-52B, and the B-52H Pylons and Pegasus adapter pylon.

Component	Material	σ_U, ksi	σ_Y, ksi	τ_U, ksi	K_{IC}, ksi$\sqrt{\text{in.}}$	C, $\frac{\text{in.}}{\text{cycle}}\left(\text{ksi}\sqrt{\text{in.}}\right)^{-m}$	m	n
B-52B front hook	Inconel 718†	175	145	135	125	0.922×10^{-11}	3.60	2.16
B-52B rear hooks	AMAX MP-35N‡	250	235	141	124	2.944×10^{-11}	3.24	1.69
Pegasus hooks	AMAX MP-35N‡	250	235	141	124	2.944×10^{-11}	3.24	1.69
Pegasus shackle	PH13-8Mo	215	199	117	122.7	21.225×10^{-11}	2.96	1.42
B-52H hooks	PH13-8Mo	215	199	117	122.7	21.225×10^{-11}	2.96	1.42
B-52H pylon front fittings	PH13-8Mo	215	199	117	122.7	21.225×10^{-11}	2.96	1.42
B-52H pylon rear fitting	PH13-8Mo	215	199	117	122.7	21.225×10^{-11}	2.96	1.42
B-52H pylon lower sway brace	PH13-8Mo	215	199	117	122.7	21.225×10^{-11}	2.96	1.42

† Inconel 718 is a registered trademark of Huntington Alloy Products Division, International Nickel Company, West Virginia.

‡ AMAX MP-35N is a trademark of SPS Technologies, Inc., Jenkintown, Pennsylvania.

Table B-2. Material properties of AMAX MP-35N alloy and PH13-8Mo stainless steel.

Material	E, lb/in^2	G, lb/in^2	ν	ρ, lb/in^3	α, in/in-°F
Inconel 718	29.6×10^6	-----	-----	0.297	6.40×10^{-6}
AMAX MP35N	34.05×10^6	11.74×10^6	0.390	0.322	7.10×10^{-6}
PH13-8Mo	28.30×10^6	11.00×10^6	0.280	0.279	5.80×10^{-6}

APPENDIX C
CALCULATIONS OF OPERATIONAL LIFE

Using the equivalent loading theory and the empirical loading theories described in the text, the safe operational numbers of flights, F_1^*, for each of the failure-critical structural components of the B-52B pylon, the Pegasus pylon, and the B-52H pylon, have been calculated using the revised Ko operational life equation. In the calculations, the initial cracks, a_c^p, were obtained from equation (2) in light of equation (7) using the proper material properties (Appendix B), the associated proof loads, V^*, and the stress-load coefficients η.

Input Data

Through the finite-element stress analysis (ref. 10), the stress-load coefficients, η, for the stress-load equations, $\sigma^* = \eta\, V^*$ [eq. (7)], for the failure-critical structural components (Appendix A) were established and are listed in Table C-1.

Table C-1. Stress-load coefficients, η, for different failure-critical structural components established from finite-element stress analysis (ref. 10)

Critical structural components	η, ksi/lb	Proof load (V^*), lb
Pegasus shackles upper parts	4.8382×10^{-3}	57,819†
Pegasus shackles lower parts	2.6444×10^{-3}	57,819†
Pegasus pylon hooks	2.4459×10^{-3}	75,000
B-52H pylon hook	0.9064×10^{-3}	83,618
B-52H pylon front fitting	0.8235×10^{-3}	136,424
B-52H pylon rear fitting	3.2097×10^{-3}	17,905
B-52H pylon lower sway brace	5.3164×10^{-3}	14,991

† Proof load for rear hooks.

Calculations of Operational Life

The following section presents detailed calculations of the operational life of various failure-critical structural components.

Pegasus Pylon Components

The operational life of Pegasus pylon components are calculated in the following.

Pegasus Pylon Adapter Shackles

For operational life calculations for the Pegasus pylon adapter shackle upper and lower parts (left and right), the values of $\{f, R^o, \bar{f}, R\}$ for the B-52B rear hooks carrying the HXLV/X43 were used (table 4). The initial cracks, a_c^p, calculated from equation (2) using the shackle proof loads are shown in Table C-1, as are the crack growths, Δa_1, calculated from equation (16), and the numbers of flights F_1^* calculated from equation (6). The key input values used were {A = 1.12, M_k = 1, a/2c = 1/4, $\sigma^* / \sigma_Y = 1$, Q = 1.2548}, with material properties listed in Appendix B.

The key data calculated for the Pegasus pylon adapter shackles are listed in Table C-2.

Table C-2. Key data for Pegasus shackles (PH13-8Mo) carrying the HXLV/X43 (40,000 lb); 90 min./flight; 3 Hz; $N_1 = 16,200$ cycles.

Pegasus shackles	V^*, lb	a_c^p, in.	f	R^o	$\bar{f}$	R	Δa_1, in.	F_1^*, flights
SUL	57,819	0.0608	0.3720	0.8158	0.3394	0.9748	1.1490×10^{-3}	69† (414)‡
SUR	57,819	0.0608	0.3328	0.8235	0.3036	0.9759	0.7753×10^{-3}	108 (675)‡
SLL	57,819	0.2051	0.3720	0.8158	0.3425	0.9540	1.4791×10^{-3}	229
SLR	57,819	0.2051	0.3328	0.8235	0.3036	0.9759	0.7754×10^{-3}	360

† Shortest operational life.

‡ If AMAX alloy is used.

Notice from Table C-2 that because of the square hole, the Pegasus pylon left shackle upper part (SUL) is the most critical structural component with the shortest safe operational life span of 69 flights. If AMAX MP-35N alloy is used instead of PH13-8Mo stainless steel for the Pegasus shackles, the numbers of operational flights, F_1^*, could be increased dramatically by 600 percent for the left shackle upper part (SUL), and by 625 percent for the right shackle upper part (SUR).

Pegasus Pylon Hooks

For the Pegasus pylon hooks carrying the HXLV/X43 system, the load data $\{f, R^o\}$ were obtained from the actual loading spectra (figs. 28~31) during taxiing of the HXLV/X43 captive flight. The SRB/DTV empirical equations (26) and (28) for the B-52B rear hooks were then used to calculate the values of $\{\bar{f}, R\}$ for the Pegasus hooks. The initial cracks, a_c^p, were calculated from equation (2) using the Pegasus hook proof loads shown in table 1, and the crack growths, Δa_1, calculated from equation (16), while the numbers of flights, F_1^*, were calculated from equation

(6). The key input values used were {A = 1.12, M_k= 1, a/2c = 1/4, $\sigma^* / \sigma_Y = 1$, Q = 1.2548}, with material properties listed in Appendix B. The key data calculated for the Pegasus pylon hooks are listed in Table C-3.

Table C-3. Key data for Pegasus pylon hooks (AMAX MP-35N) carrying HXLV/X43 (40,000 lb); 90 min./flight; 3 Hz; N_1 = 16.200 cycles.

Pegasus hooks	V^*, lb	a_c^p, in.	f	R^o	$\overline{f}$	R	Δa_1, in.	F_1^*, flights
VPFL	75,000	0.1455	0.4585	0.8571	0.4183	0.9805	0.2213-3	658
VPFR	75,000	0.1455	0.4747	0.8409	0.4331	0.9782	0.2991-3	504†
VPRL	75,000	0.1455	0.2607	0.7647	0.2379	0.9678	0.0830-3	2,292
VPRR	75,000	0.1455	0.2966	0.7948	0.2706	0.9719	0.1001-3	1,827

† Shortest life.

Note from Table C-3 that among the four Pegasus pylon hooks, the front right hook (VPFR) has the shortest operational life of 504 flights.

B-52H Pylon Components

The following sections show how to apply the empirical loading theories developed in the text for preflight operational life analysis of B-52H pylon carrying X-37. Because there are no actual flight data available for B-52H carrying the X-37 vehicle (fig. 3), the past flight data of X-38 drop test vehicle (16,557 lb) and the empirical loading theory developed based on SRB/DTV (49,000 lb) flight data had to be used for the pre-flight estimations of the operational life spans of B-52H pylon critical structural components.

X-38 Drop Test Vehicle Hooks Data

From the X-38 Drop Test Vehicle hooks actual loading spectra during taxiing and landing, the values of operational load ratio V_{max}^o / V_S (maximum load-static load) associated with the worst load cycles were determined as

Table C-4. Load ratio $\{V_{max}^{o} / V_S\}$ obtained from the X-38 (16,557 lb) taxiing-landing data.

	V_{max}^{o} / V_S	
X-38 hooks	Taxiing	Landing
Front hook	1.1708	1.2690
Rear hook	1.0667	1.2678

Determinations of Both Load Factor and Stress (Load) Ratio Associated with the Constant-Amplitude Loading Factor

The static loads V_S (with preloads) for the B-52H pylon hooks (carrying the X-37 vehicle) are V_S = 21,157 lb for the front hook and V_S = 27,037 lb for the rear hook. Based on those hook static loads, the maximum operating loads, V_{max}^{o}, for the B-52H pylon components have been estimated using the data given in table A-3 and the following equations.

$$f = \frac{V_{max}^{o}}{V^*}; R^o = 2\frac{V_S}{V_{max}^{o}} - 1 \tag{C-1}$$

The calculated data for the operational loading of the B-52H pylon components carrying the X-37 vehicle are listed in Tables C-5 and C-6. Notice that the values of $\{f, R^o\}$ for the B-52H rear hook were also used for the rest of B-52H pylon components.

Table C-5. Load values for the B-52H airplane carrying the X-37 vehicle (7,000 lb) based on X-38 vehicle taxiing data.

B-52H pylon parts	V^*, lb	V_S, lb	(V_{max}^{o} / V_S) †	V_{max}^{o}, lb	f	R^o
Front hook(HF)	83,618	21,157	1.1708	24,770	0.2962	0.7083
Rear hook(HR)	83,618	27,037	1.0667	28,840	0.3449	0.8750
Front fitting(FF)					0.3449	0.8750‡
Rear fitting (RF)					0.3449	0.8750‡
Lower sway brace (HLSB)					0.3449	0.8750‡

† X-38 taxiing data.

‡ Rear hook values.

Table C-6. Load values for the B-52H airplane carrying the X-37 vehicle (7,000 lb) based on X-38 vehicle landing data.

B-52H pylon parts	V^*, lb	V_S, lb	(V^o_{max}/V_S) †	V^o_{max}, lb.	f	R^o
Front hook (HF)	83,618	21,157	1.2690	26,848	0.3211	0.5761
Rear hook (HR)	83,618	27,037	1.2678	34,278	0.4099	0.5775
Front fitting (HFF)					0.4099‡	0.5775‡
Rear fitting (HRF)					0.4099‡	0.5775‡
Lower sway brace (HLSB)					0.4099‡	0.5775‡

† X-38 landing data.

‡ Rear hook values.

After the $\{f, R^o\}$ values have been determined, the empirical equations (26) and (28) (established from the SRB/DTV flight data) may be used to calculate the unknown values of $\{\bar{f}, R\}$ for the equivalent constant amplitude loading spectra for the B-52H pylon carrying the X-37 vehicle. The resulting data are listed in table C-7 for both taxiing and landing. Again $\{\bar{f}, R\}$ values of the B-52H rear hook were also used for the front fitting, rear fittings, and lower sway brace.

Table C-7. Values of $\{\bar{f}, R\}$ calculated for B-52H pylon parts carrying the X-37 vehicle.

B-52H pylon part	Taxiing		Landing	
	$\bar{f}$	R	$\bar{f}$	R
Front hook (HF)	0.2703	0.9601	0.2930	0.9420
Rear hook (HR)	0.3147	0.9829	0.3740	0.9422
Front fitting (HFF)	0.3147‡	0.9829‡	0.3740‡	0.9422‡
Rear fitting (HRF)	0.3147‡	0.9829‡	0.3740‡	0.9422‡
Lower sway brace (HLSB)	0.3147‡	0.9829‡	0.3740‡	0.9422‡

‡ Rear hook values.

Numbers of Flights

The flight duration of the B-52H carrying the X-37 vehicle was assumed to be 50 min. (similar to the SRB/DTV case) with 4 Hz loading cycles (i.e., $N_1 = 50 \times 60 \times 4 = 12{,}000$ cycles). Making use of the appropriate material data in Appendix, the values of the proof loads, V^*, and the associated stress-load coefficients, η, (table 1), the initial crack size, a_c^p ,can be calculated from equation (2) [in light of eq. (7)] for each structural component. Then, making use of the additional data of $\{\bar{f}, R\}$ given in table C-7, and the values of N_1 =12,000 cycles, the crack growth, Δa_1, for each B-52H pylon critical component may be calculated from equation (16).

Finally the operational life, F_1^*, for each structural component may be calculated from equation (6) using the operational load factor, *f*, obtained from the loading spectra. The results are listed in the following tables C-8 and C-9.

1. Based on the X-38 Vehicle Taxiing Data

Table C-8. Key .data for B-52H pylon parts (PH13-8Mo) carrying the X-37 vehicle (7,000 lb); 50 min./flight; 3 Hz; N_1 = 12,000 cycles; based on X-38 taxiing.

Name	V^*, lb	a_c^p, in.	f	R^o	$\bar{f}$	R	Δa_1, in.	F_1^*, flights
HF	123,198	0.3844	0.2011	0.7083	0.1835	0.9601	0.2647-3	2.381†
HR	123,198	0.3844	0.2341	0.8750	0.2136	0.9829	0.1246-3	4,820
HFF	135,600	0.3844	0.2341	0.8750	0.3147	0.9829	0.1246-3	4,820
HRF	34,791	0.3844	0.2341	0.8750	0.3147	0.9829	0.1246-3	4,820
HLSB	21,004	0.3844	0.2341	0.8750	0.3147	0.9829	0.1246-3	4,820

† Shortest life.

2. Based on X-38 Drop Test Vehicle Landing Data

Table C-9. Key data for B-52H pylon parts (PH13-8Mo) carrying X-37 (7,000 lb); 50 min flight; 3Hz; N_1 = 12,000 cycles; based on X-38 landing.

Name	V^*, lb	a_c^p, in.	f	R^o	$\bar{f}$	R	Δa_1, in.	F_1^*, flights
HF	123,198	0.3844	0.2179	0.5761	0.1988	0.9420	0.5706-3	1,079†
HR	123,198	0.3844	0.2782	0.5775	0.2538	0.9422	1.1700-3	485
HFF	135,600	0.3844	0.2782	0.5775	0.2538	0.9422	1.1700-3	485
HRF	34,791	0.3844	0.2782	0.5775	0.2538	0.9422	1.1700-3	485
HLSB	21,004	0.3844	0.2782	0.5775	0.2538	0.9422	1.1700-3	485

† Longest life.

Note from tables C-8 and C-9 that the B-52H pylon front hook has the shortest operational life, 2,381 flights for the taxing case, but the longest operational life of 1,079 flights for the landing case. Keep in mind that the operational life spans presented in tables C-8 and C-9 are the preflight-estimated values using X-38 data, and are subjected to updating once the actual flight loading spectra of the B-52H pylon carrying the X-37 are available.

Summary of Operational Flights

The safe operational numbers of flights, F_1^*, for the failure-critical structural components of the B-52B pylon, the Pegasus pylon, and B-52H pylon are summarized in tables C-10 and C-11.

Table C-10. Safe operational flights, F_1^*, for Pegasus pylon components carrying the HXLV/X-43 system (40,000 lb, 90 min./flight).

Pegasus pylon	F_1^*, flights
Shackle upper part left (SUL)	69† (414)‡
Shackle upper part right (SUR)	108 (675)‡
Shackle lower part left (SLL)	229
Shackle lower part left (SLR)	360
Front left hook (VPFL)	658
Front right hook (VPFR)	504
Rear left hook (VPRL)	2,292
Rear right hook (VPRR)	1,827

† Shortest operational life.

‡ If AMAX is used.

Table C-11. Safe operational flights, F_1^*, for B-52H pylon components carrying the X-37 (7000 lb) approach/landing vehicle; 50 min./flight; 4Hz.

B-52H pylon parts	F_1^*, flights	
	Based on X-38 taxiing	Based on X-38 landing
Front hook (HF)	2,381†	1,079‡
Rear hook (HF)	4,820	485
Front fitting (HFF)	4,820	485
Rear fitting (HRF)	4,820	485
Lower sway brace (HLSB)	4,820	485

† Shortest life for taxiing case.

‡ Longest life for landing case.

REFERENCES

1. Ko, W. L., A. L. Carter, W. W. Totton, and J. M. Ficke, *Application of Fracture Mechanics and Half-Cycle Method to the Prediction of Fatigue Life of B-52 Aircraft Pylon Components*, NASA/TM-88277, September 1989.

2. Ko, William L., *Prediction of Service Life of Aircraft Structural Components Using the Half-Cycle Method*, NASA TM-86812, May 1987. Also in Folias, E.S., *International Journal of Fracture*, Vol. 39, pp. 44–62, Kluwer Academic Publishers, 1989.

3. Ko, William L., Richard Monaghan, *Practical Theories for Service Life Prediction of Critical Aerospace Structural Components*, NASA/TM-4354, 1992.

4. Ko, William L. and Richard Monaghan, and Raymond H. Jackson "Practical Theories for Service Life Predictions of Critical Aerospace Structural Components" Presented at the *4th International Conference on Failure, Product Liability and Technical Insurance,* Vienna, Austria, July 6-9, 1992. Elsevier Science Publishers, July 1993.

5. Ko, William L., *Aging Theories for Establishing the Safe Life Span of Airborne Critical Structural Components*, NASA/TP-2003-212034, December 2003.

6. Barrois, W. and E. L., Ripley, eds, *Fatigue of Aircraft Structures*, Macmillan Co., New York, 1963.

7. Ko, William L. and Leslie Gong, *Thermostructural Analysis of Unconventional Wing Structures of a Hyper-X Hypersonic Flight Research Vehicle for the Mach 7 Mission*, NASA/TP 2001-210398, October 2001.

8. Ko, William L., *Stress Analysis of B-52 Pylon Hooks for Carrying the X-38 Drop Test Vehicle*. NASA/TM-97-206218, October 1997.

9. Ko, William L. and Lawrence S. Schuster, *Stress Analysis of B-52 Pylon Hooks*, NASA/ TM-84924, October 1985.

10. Ko, William L., *Stress Analysis of B-52B/B-52H Air-Launching Systems Failure Critical Structural Components*, NASA/TP-2005-212862, 2005.

FIGURES

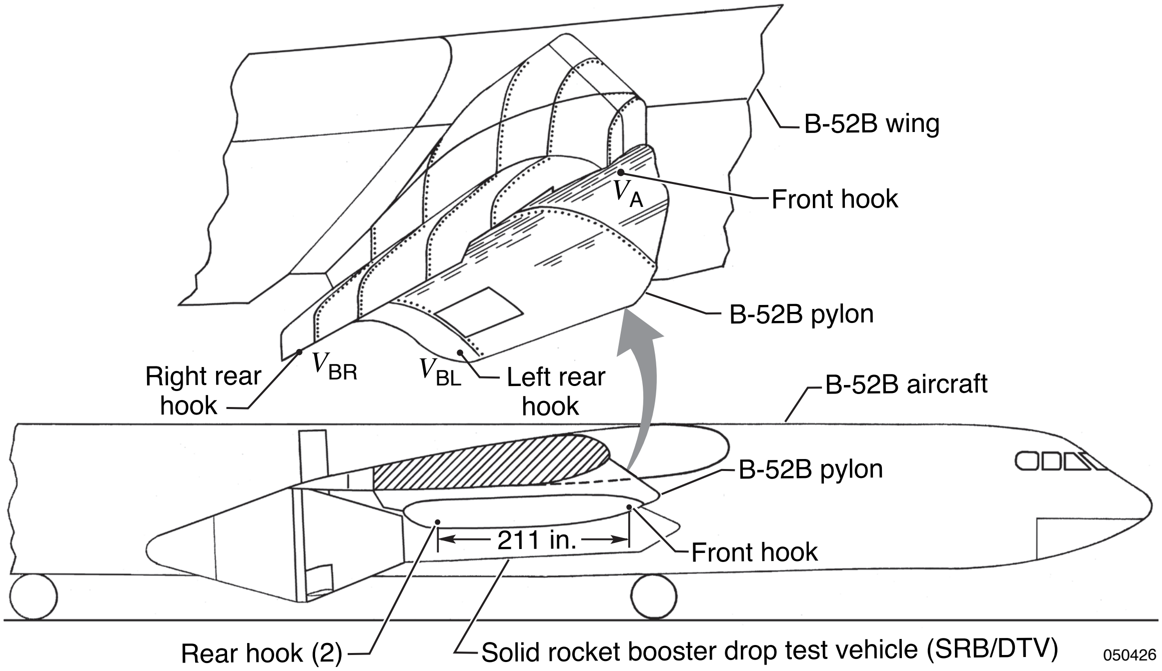

Figure 1. The B-52B aircraft carrying the solid rocket booster drop test vehicle (SRB/DTV, 49,000 lb).

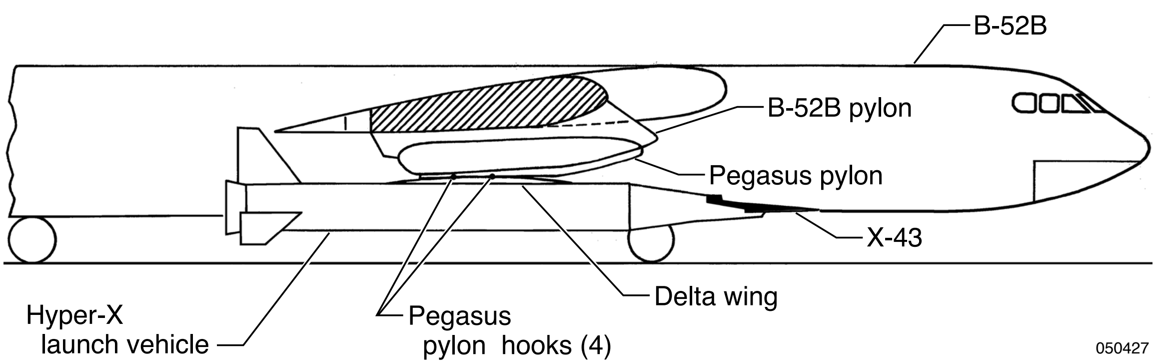

Figure 2. The B-52-B aircraft carrying the winged HXLV/X-43 system (40,000 lb).

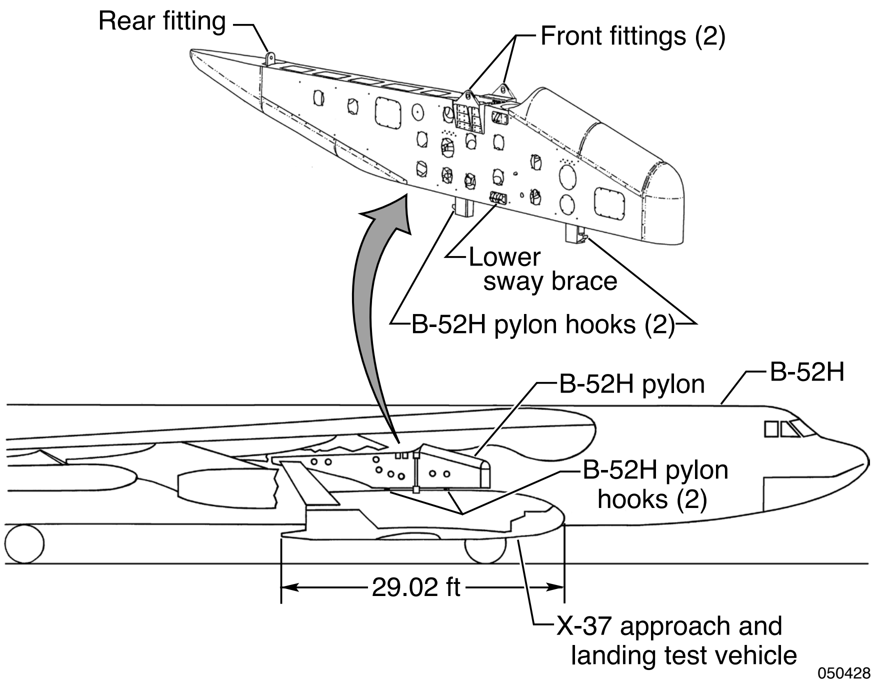

Figure 3. The B-52H aircraft carrying the X-37 approach and landing test vehicle (7,000 lb).

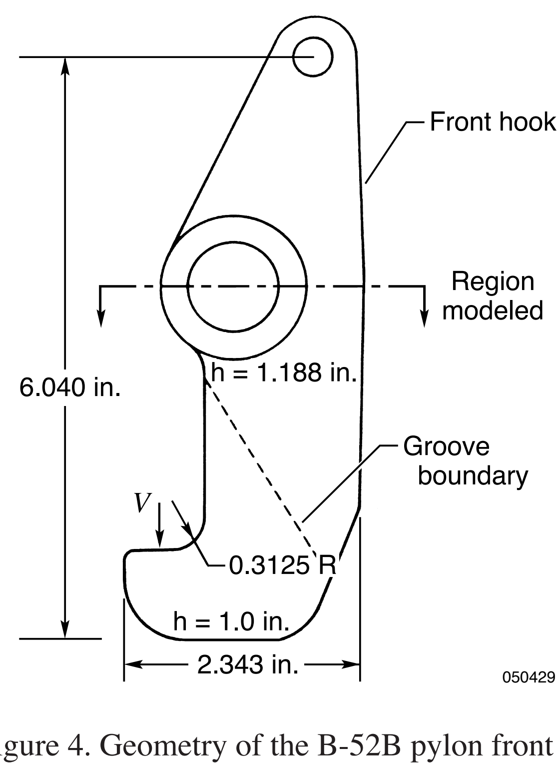

Figure 4. Geometry of the B-52B pylon front hook.

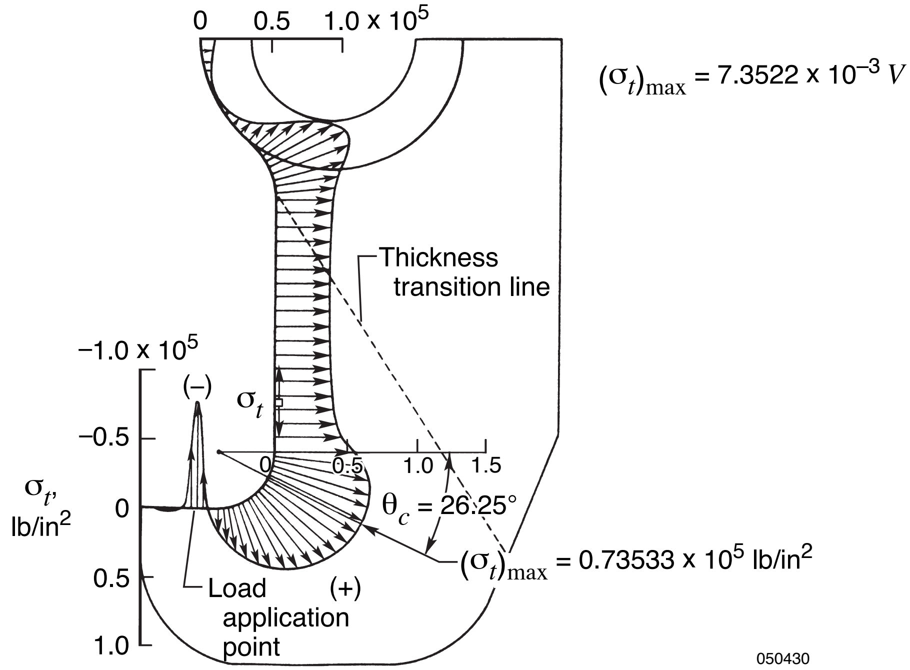

Figure 5. Distribution of tangential stress, σ_t, along inner boundary of B-52B pylon front hook; V= 10,000 lb

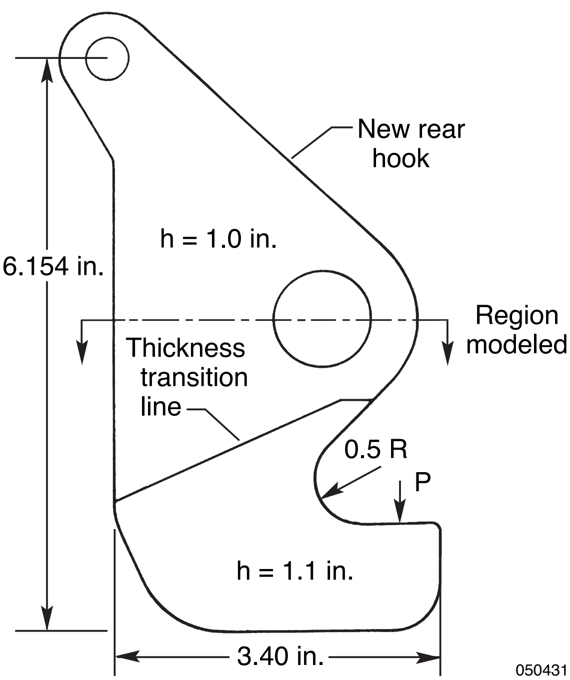

Figure 6. Geometry of the B-52B pylon rear hook.

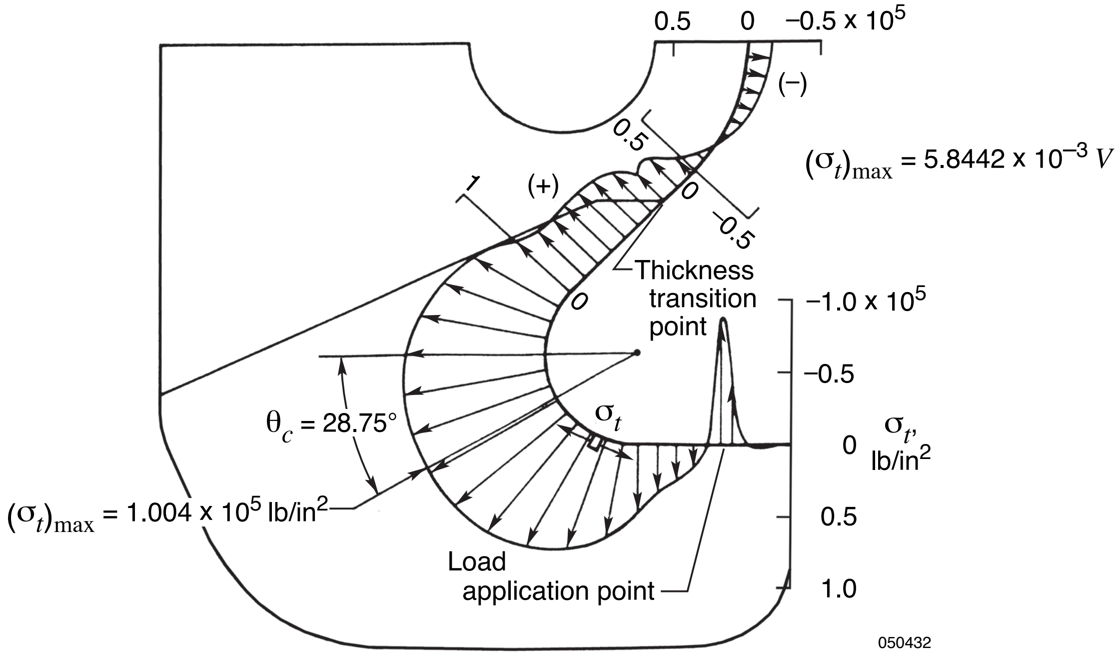

Figure 7. Distribution of tangential stress, σ_t , along the inner boundary of the B-52B pylon rear hook; V= 17,179.53 lb

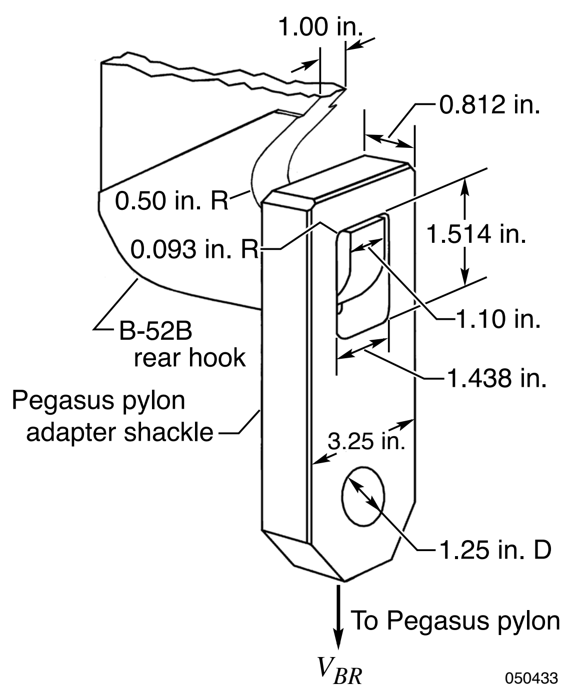

Figure 8. Geometry of the Pegasus pylon adapter shackle connected to the B-52B pylon rear hook.

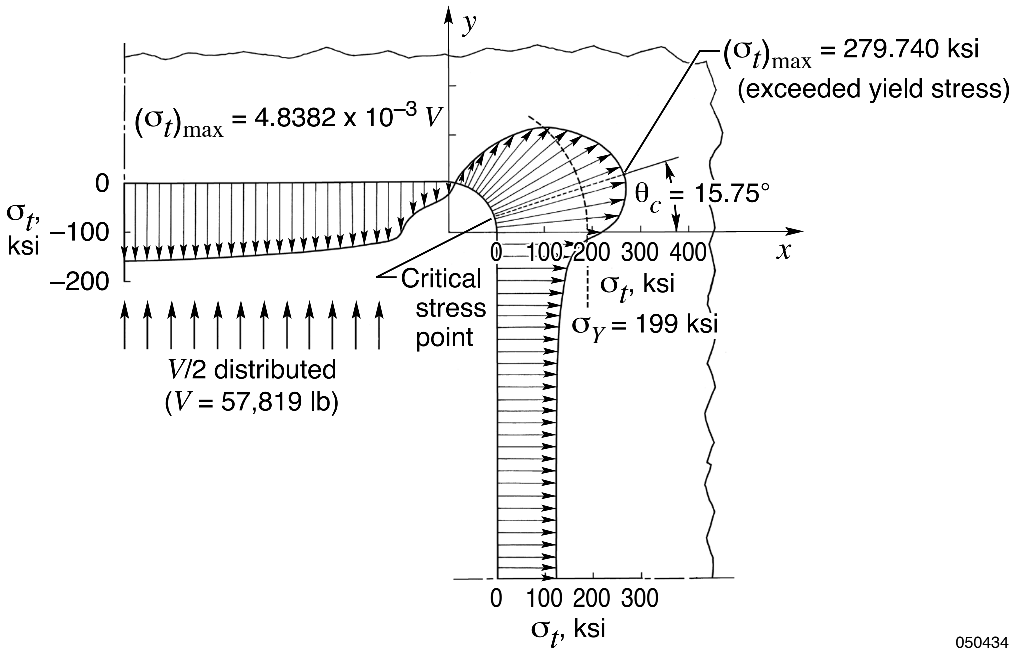

Figure 9. Distribution of tangential stresses, σ_t , along the inner boundary of the Pegasus pylon adapter shackle upper part.

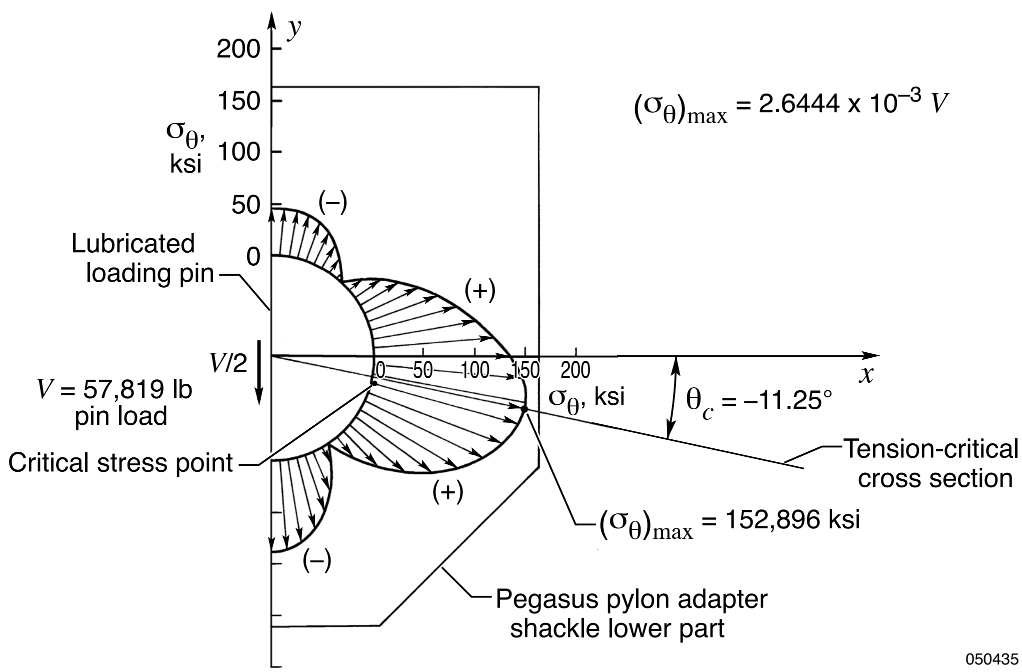

Figure 10. Distribution of tangential stresses, σ_θ, along the hole boundary of the Pegasus pylon adapter shackle lower part.

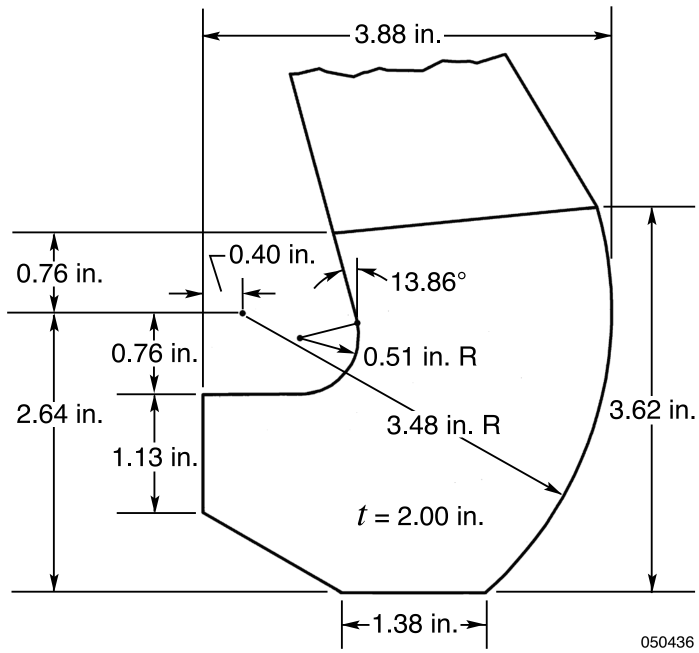

Figure 11. Geometry of the Pegasus pylon hook; dimensions in inches.

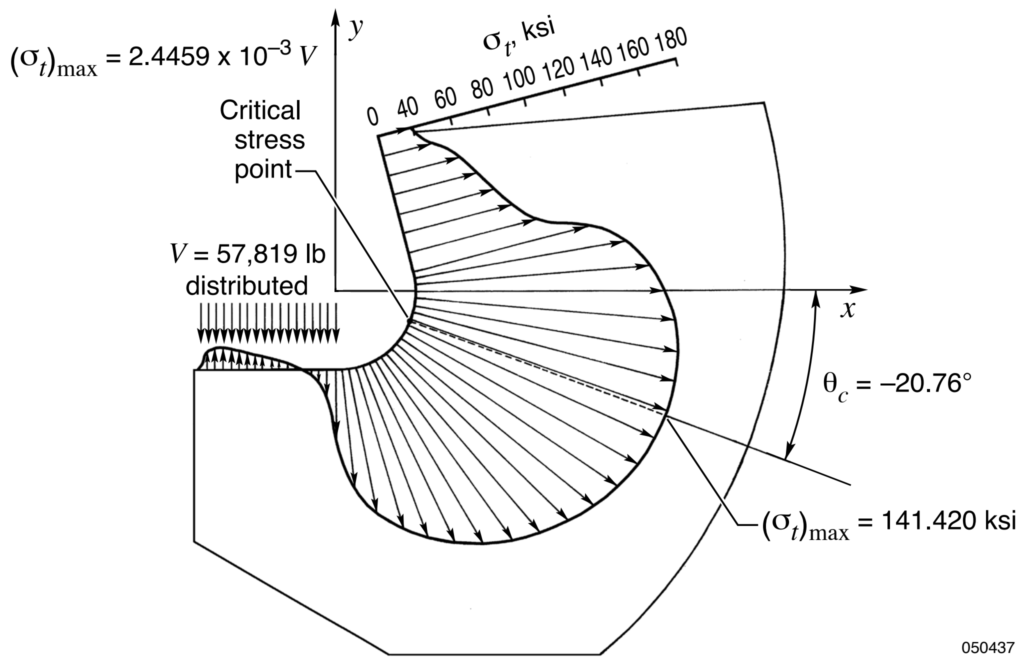

Figure 12. Distribution of tangential stress, σ_t, along the inner boundary of the Pegasus pylon hook.

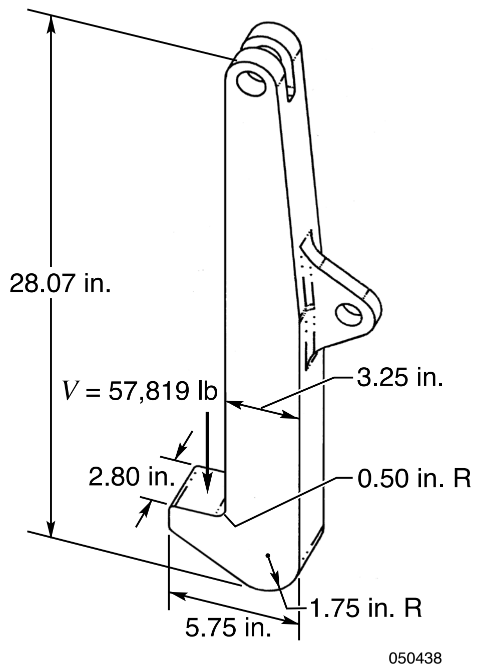

Figure 13. Geometry of the B-52H pylon hook.

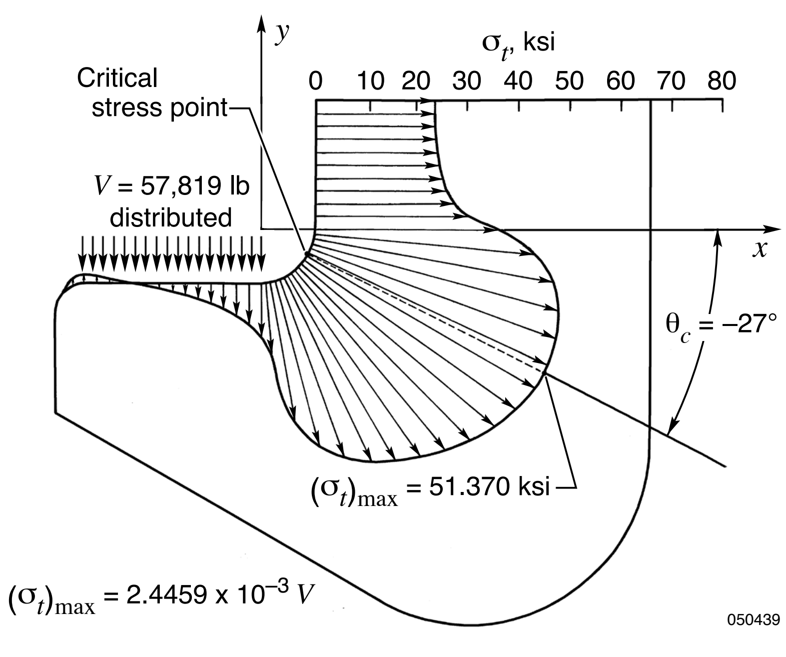

Figure 14. Distribution of tangential stress, σ_t , along the inner boundary of the B-52H hook.

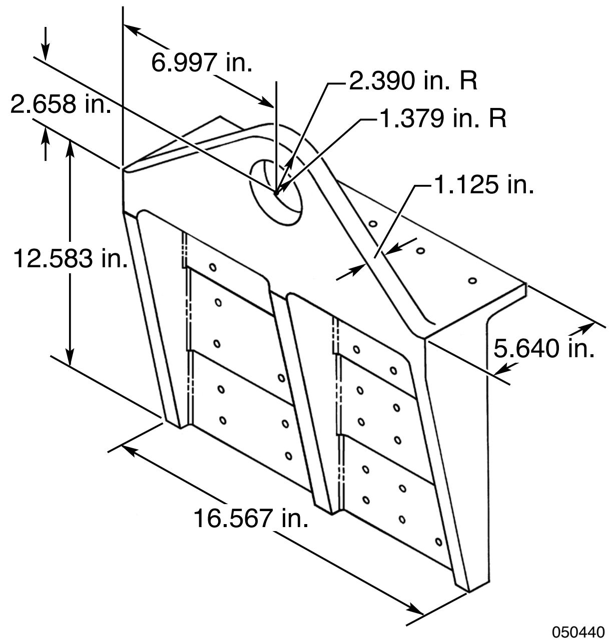

Figure 15. The B-52H pylon front fitting.

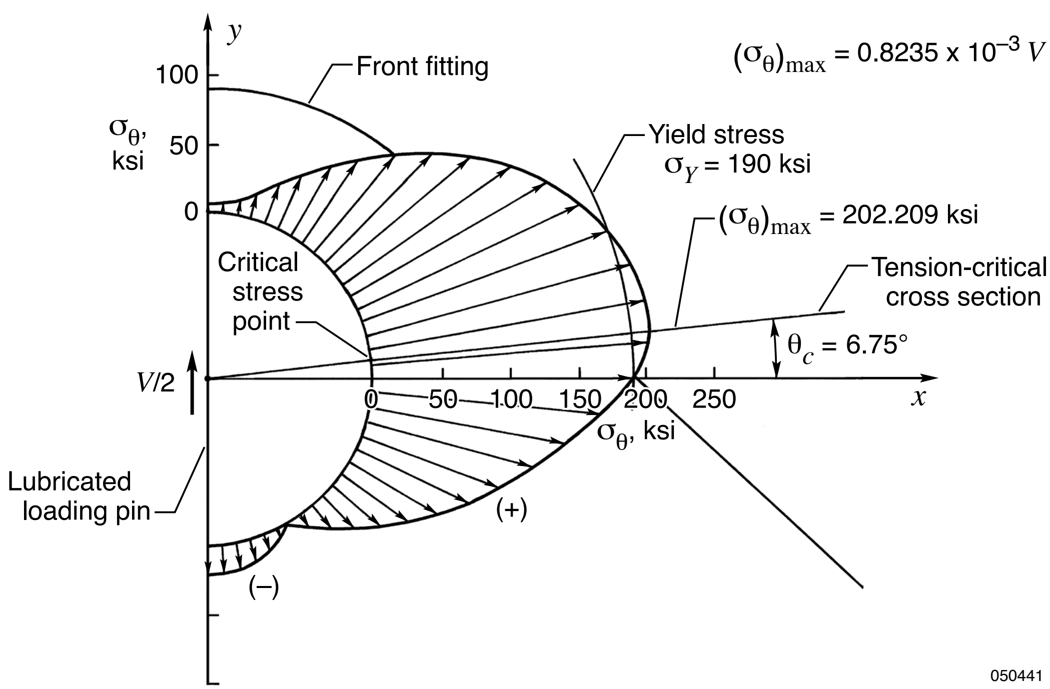

Figure 16. Distribution of tangential stress, σ_θ, along the hole boundary of the B-52H pylon front fitting.

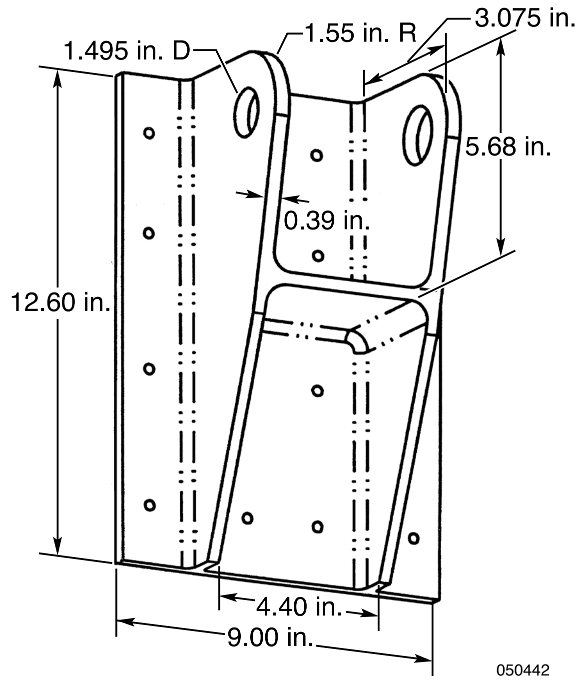

Figure 17. The B-52H pylon rear fitting.

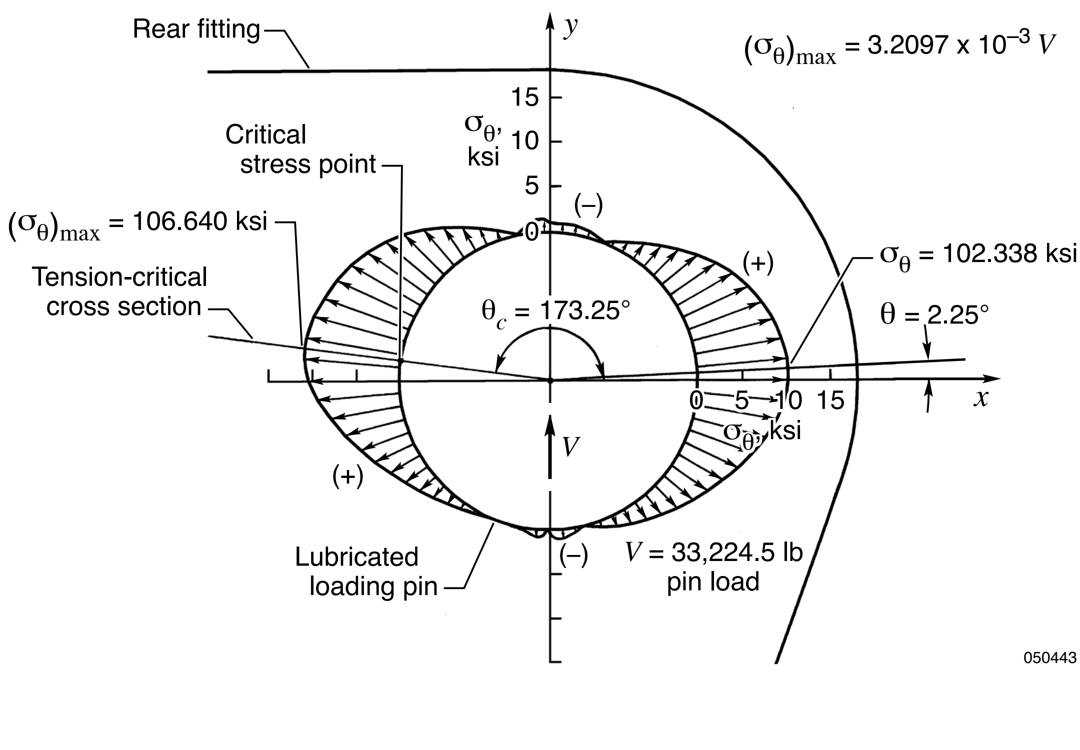

Figure 18. Distribution of tangential stress, σ_θ, along the hole boundary of the B-52H pylon rear fitting.

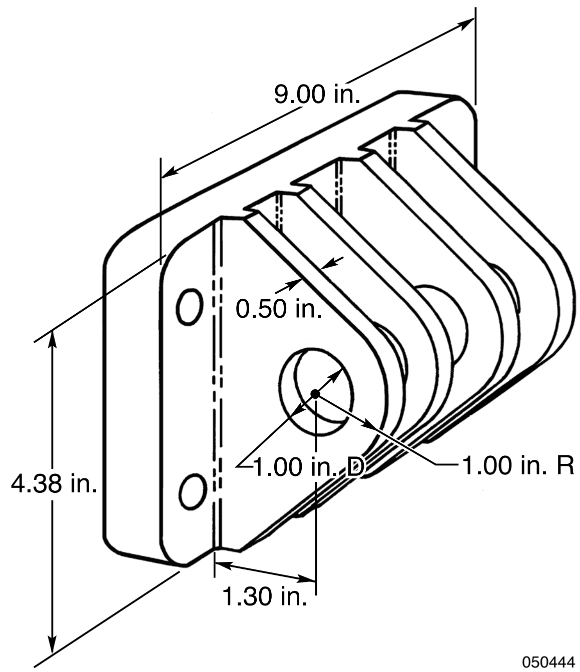

Figure 19. The B-52H pylon lower sway brace.

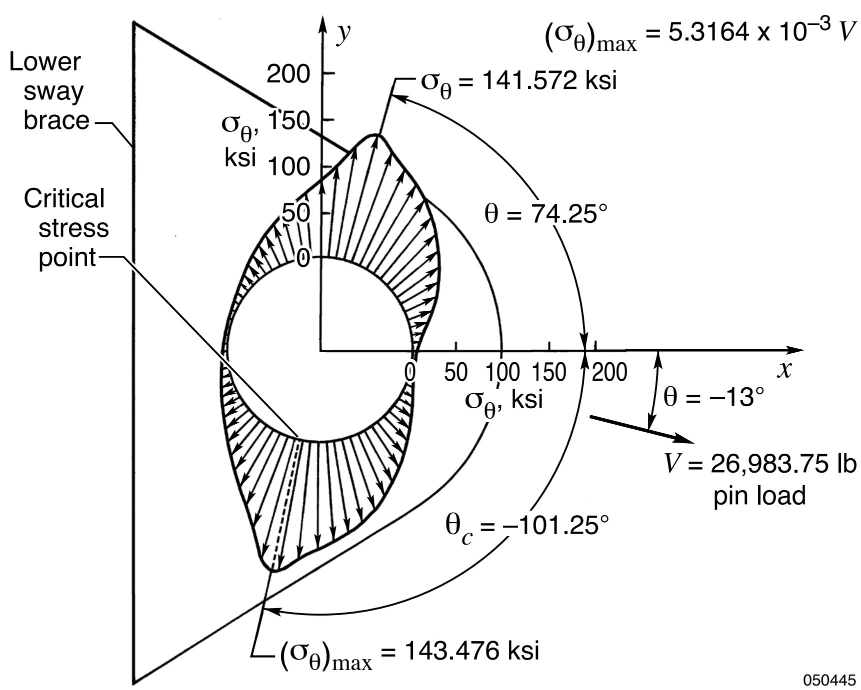

Figure 20. Distribution of tangential stress, σ_θ, along the hole boundary of the B-52H pylon lower sway brace.

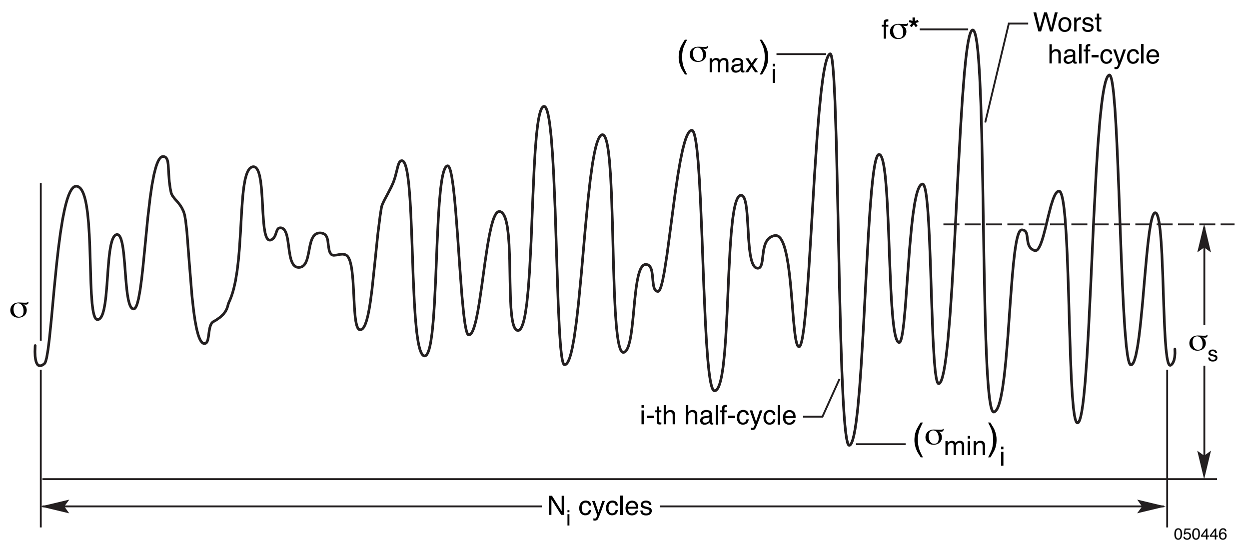

Figure 21(a). Random stress cycles.

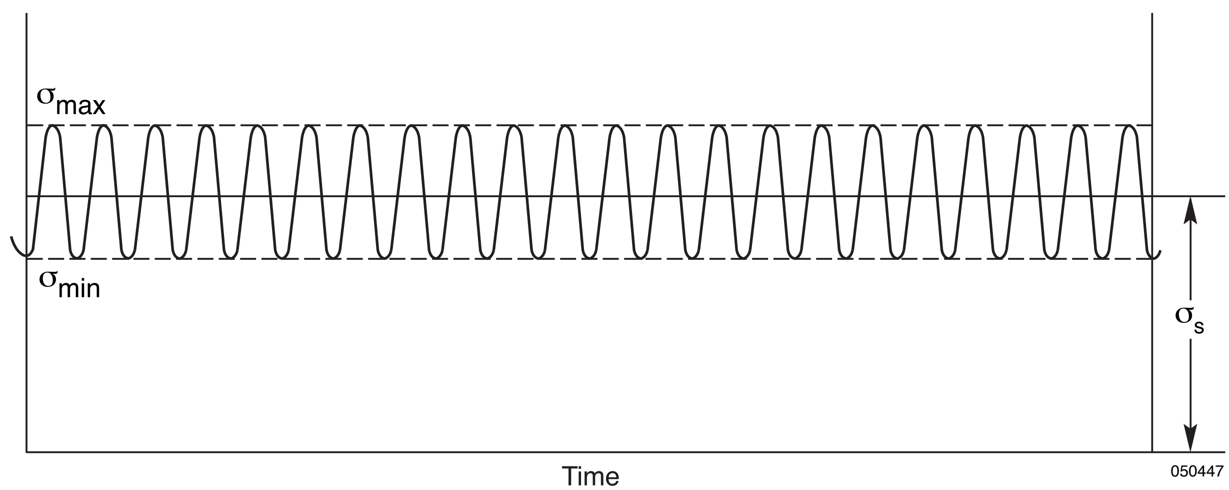

Figure 21(b). Representation of the random loading spectrum with the equivalent-constant-amplitude loading spectrum; both loading spectra induce identical crack growth, Δa_1 .

Figure 21. Random Stress cycles and load spectra.

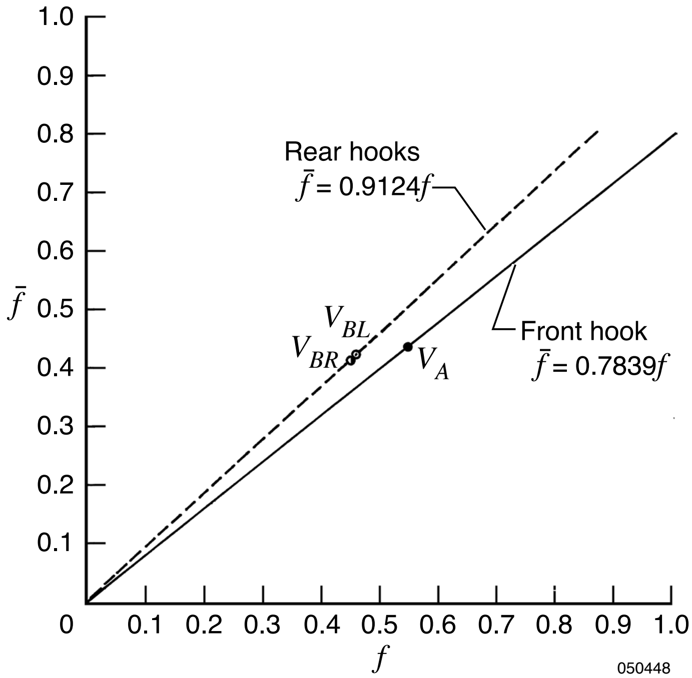

Figure 22. Plots of equivalent load factors, f, as functions of operational load factor, $\bar{f}$, for the B-52B pylon hooks; SRB/DTV flight data.

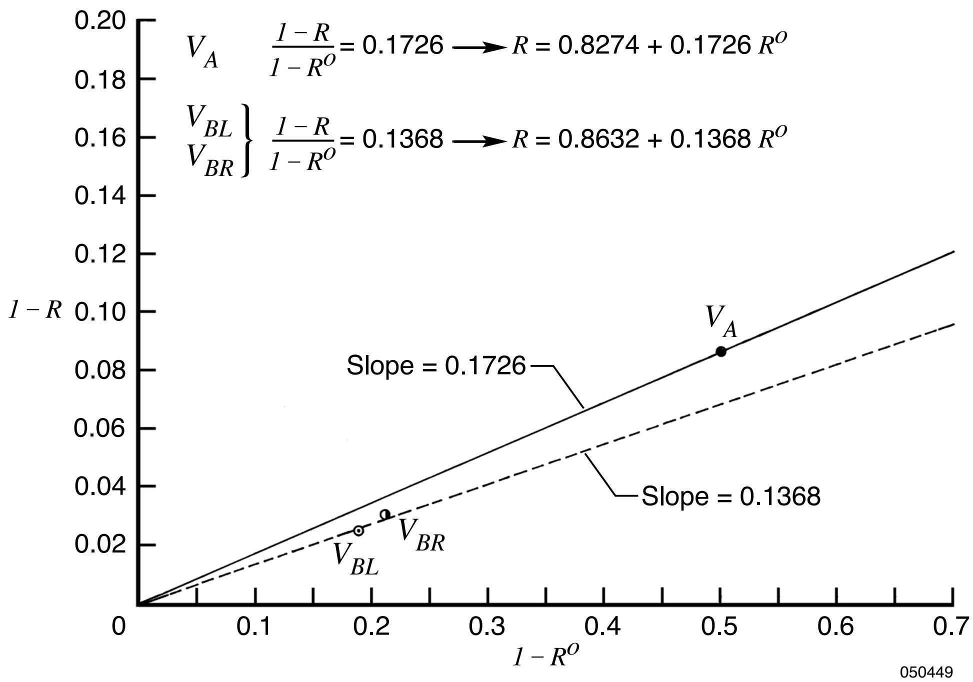

Figure 23. Plot of equivalent stress ratio $(1-R)$ as a function of operational stress ratio $(1-R^O)$ for the B-52B pylon hooks; SRB/DTB flight data.

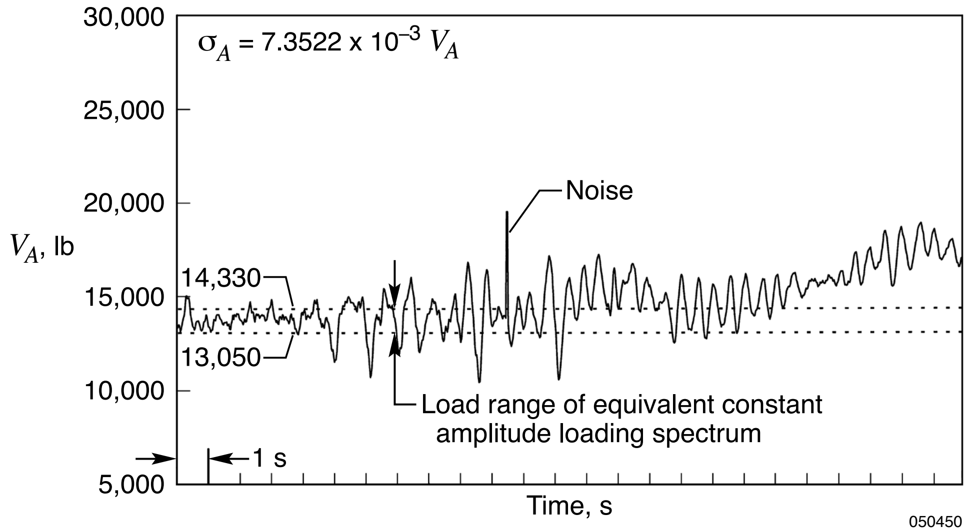

Figure 24. Loading spectrum of the B-52B front hook (V_A) carrying the HXLV/X-43 system during takeoff.

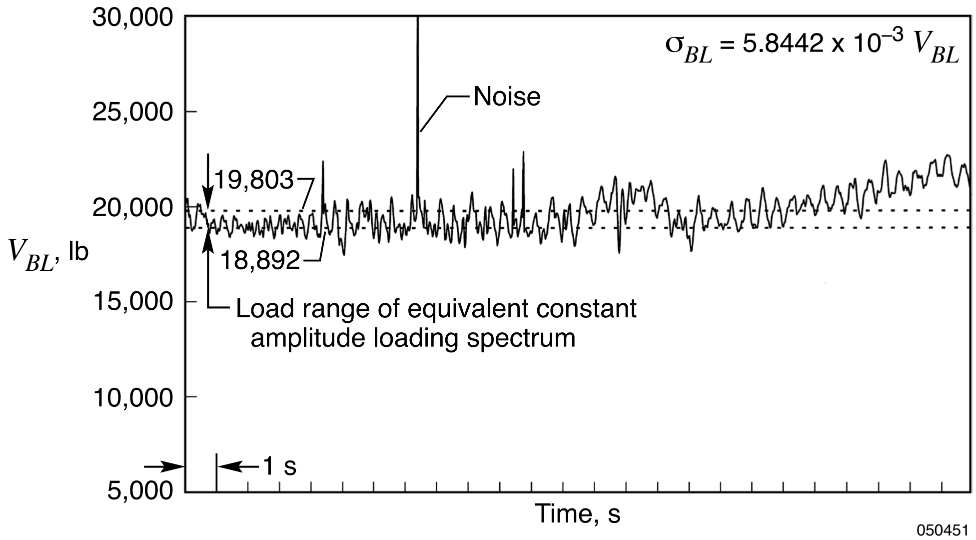

Figure 25. Loading spectrum of the B-52B front hook (V_A) carrying the HXLV/X-43 system during takeoff.

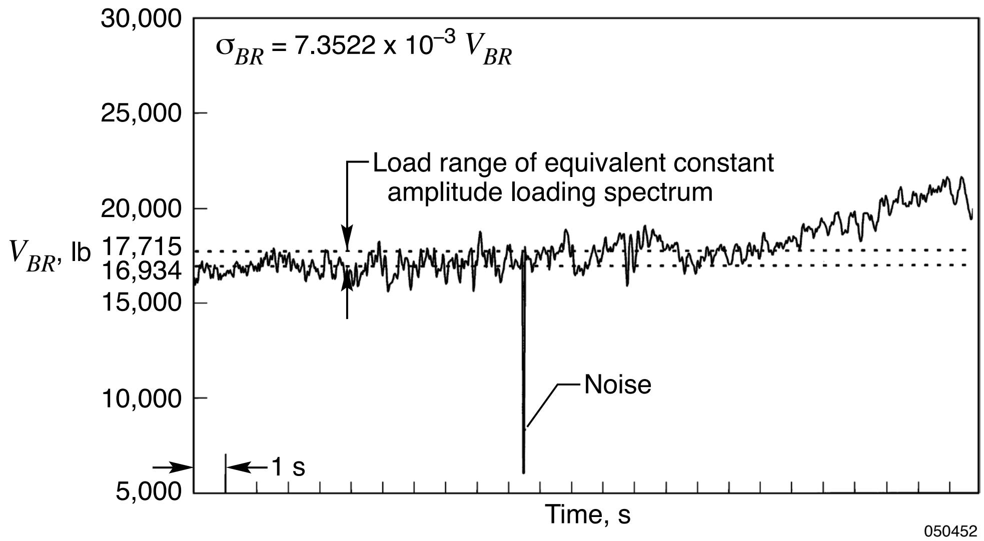

Figure 26. Loading spectrum of the B-52B rear left hook (V_{BL}) carrying the HXLV/X-43 system during takeoff.

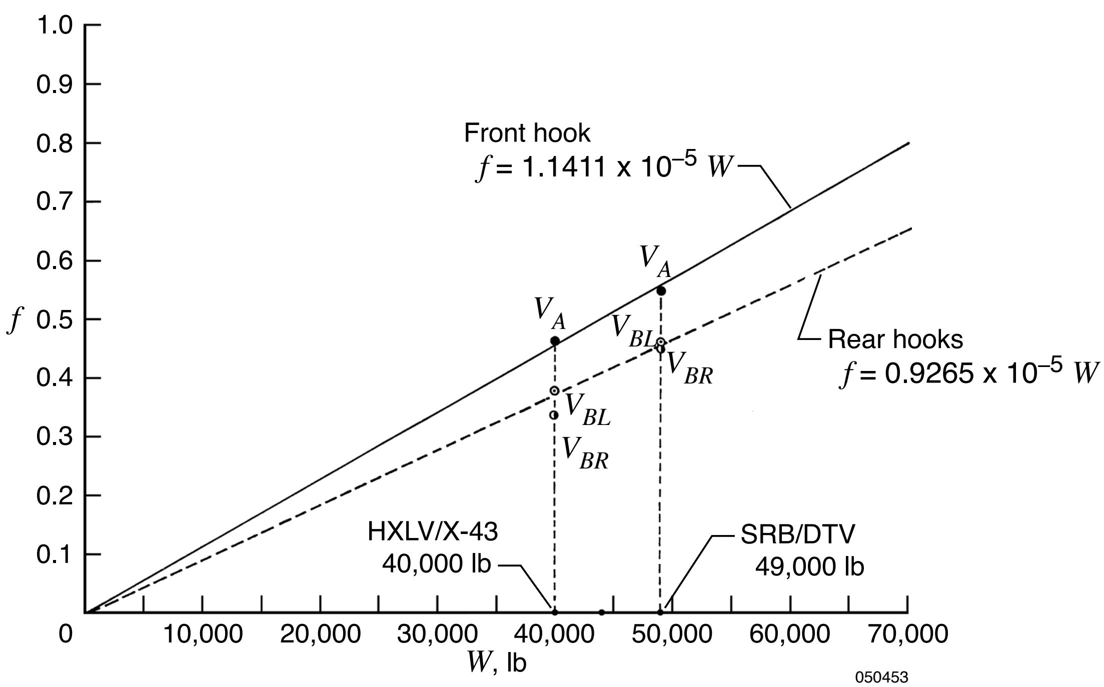

Figure 27. Plots of operational load factors, f, as functions of store weight, W, for the B-52B pylon hooks; SRB/DTV and the HXLV/X-43 flight data.

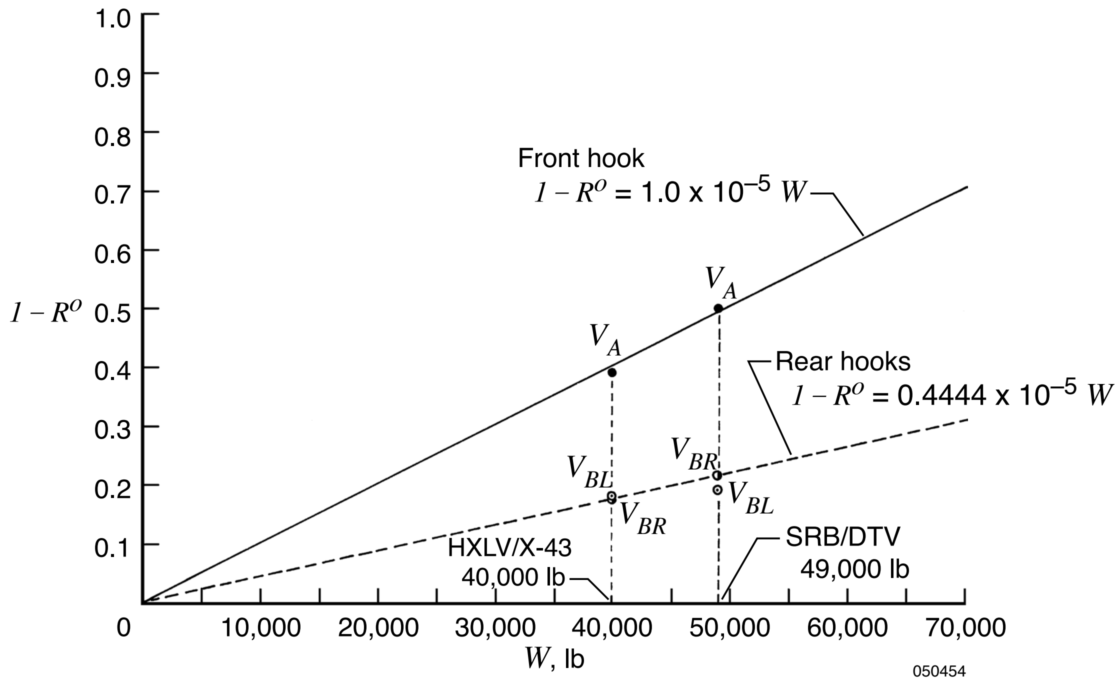

Figure 28. Plots of stress ratios $(1 - R^o)$ as functions of store weight, W, for the B-52B pylon hooks; SRB/DTV and the HXLV/X-43 flight data.

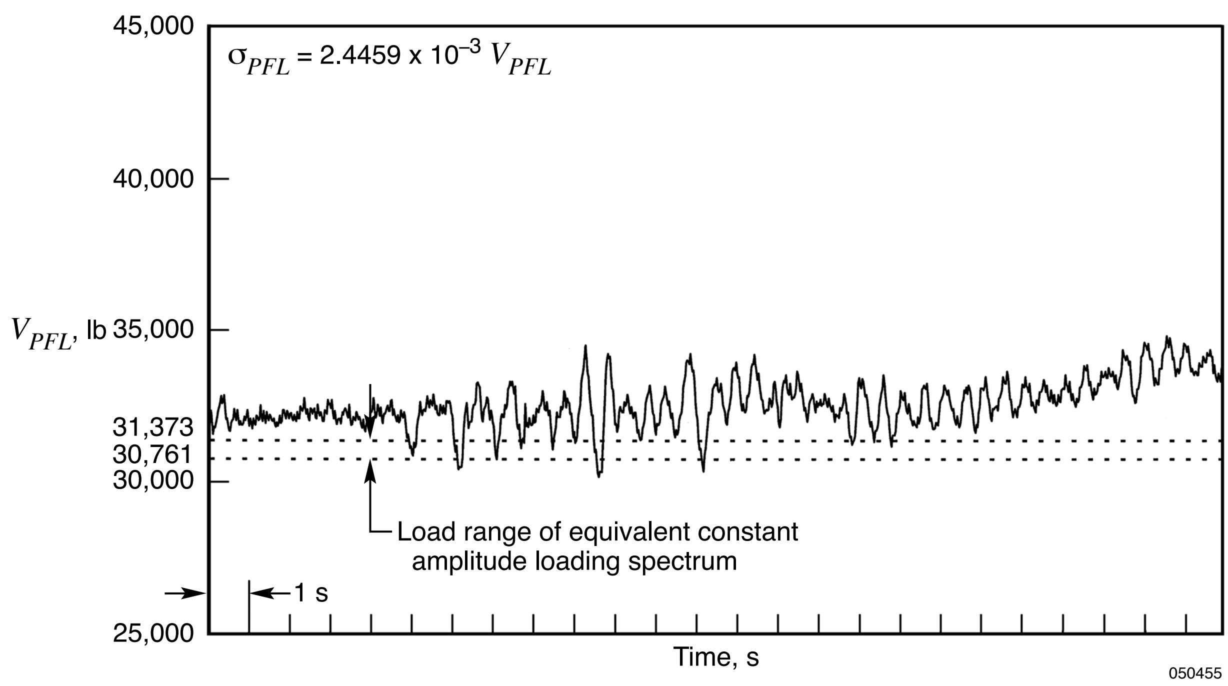

Figure 29. Loading spectrum of the Pegasus pylon front left hook carrying the HXLV/X-43 during taxiing.

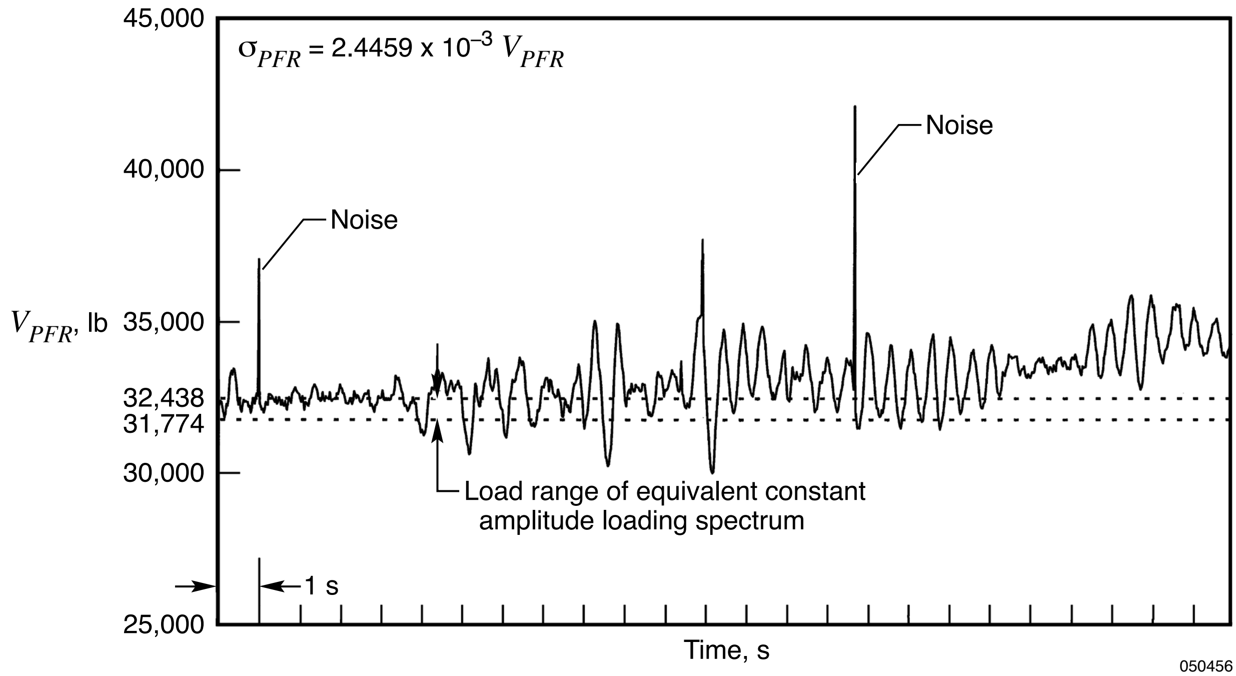

Figure 30. Loading spectrum of the Pegasus pylon front right hook carrying the HXLV/X-43 during taxiing.

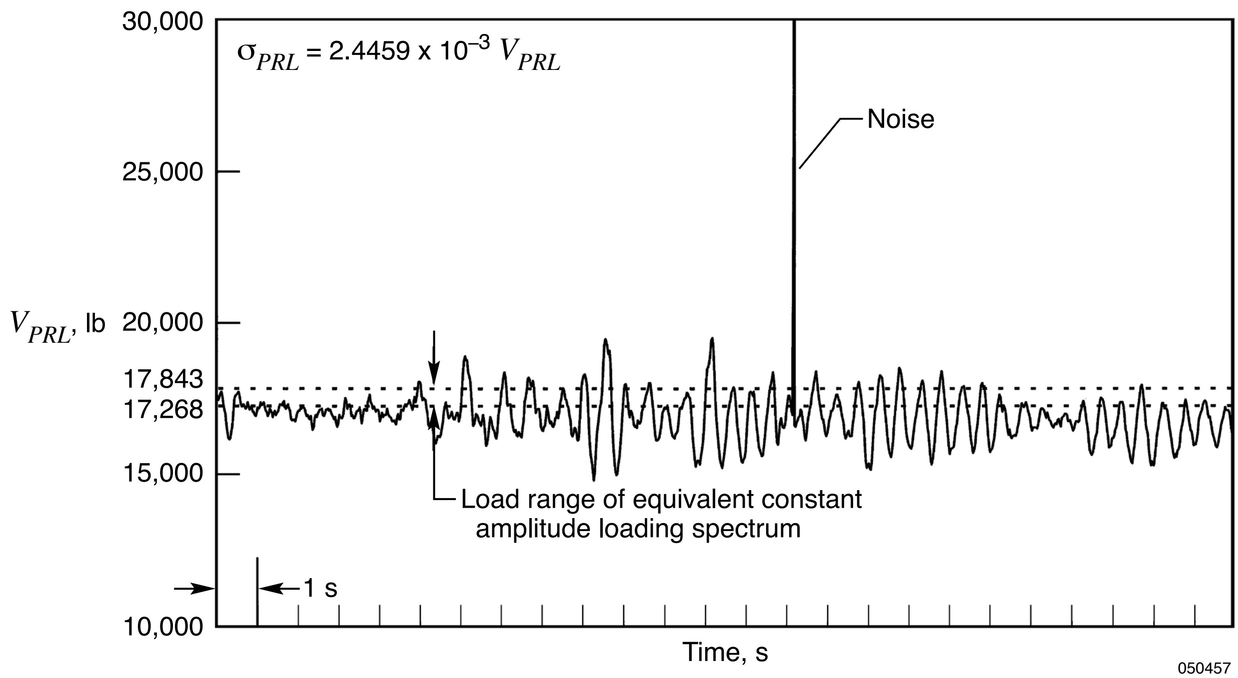

Figure 31. Loading spectrum of the Pegasus pylon rear left hook carrying the HXLV/X-43 during taxiing.

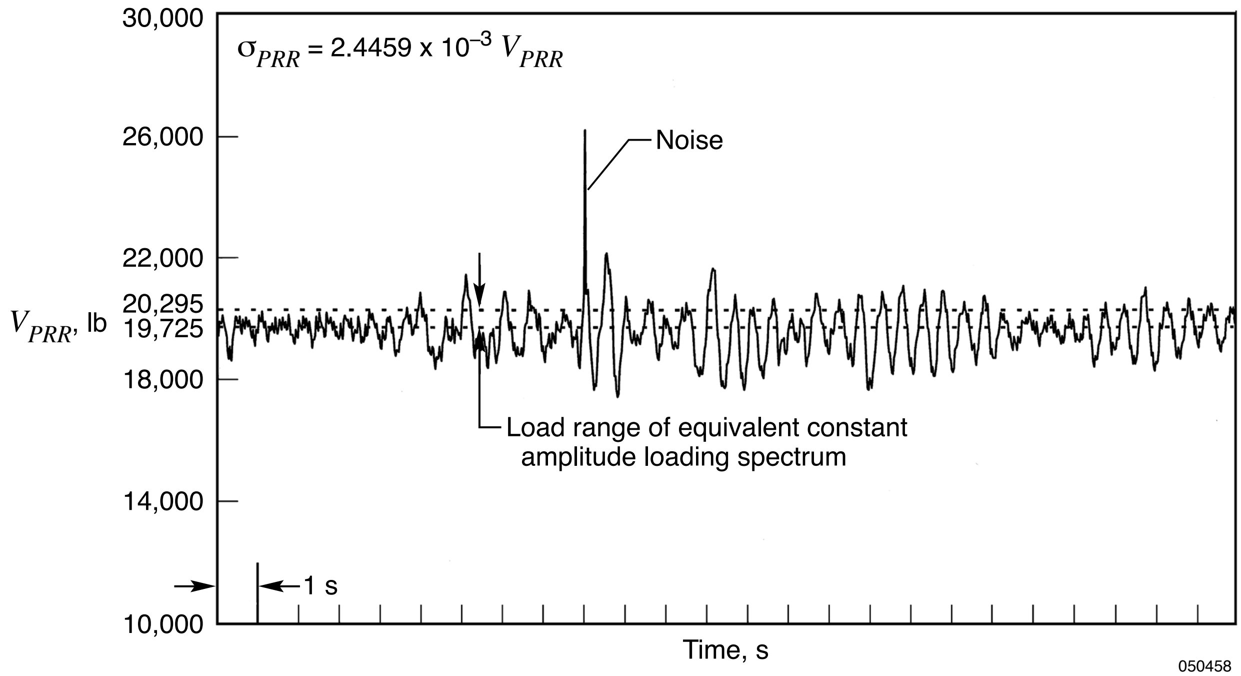

Figure 32 Loading spectrum of the Pegasus pylon rear right hook carrying the HXLV/X-43 during taxiing.

REPORT DOCUMENTATION PAGE	*Form Approved* *OMB No. 0704-0188*

1. REPORT DATE *(DD-MM-YYYY)*
15-05-2006

2. REPORT TYPE
Technical Publication

3. DATES COVERED *(From - To)*

4. TITLE AND SUBTITLE
Extended Aging Theories for Predictions of Safe Operational Life of Critical Airborne Structural Components

5a. CONTRACT NUMBER

5b. GRANT NUMBER

5c. PROGRAM ELEMENT NUMBER

6. AUTHOR(S)
Ko, William L., Chen, Tony

5d. PROJECT NUMBER

5e. TASK NUMBER

5f. WORK UNIT NUMBER
24-104-08-01 SE RR 00 000

7. PERFORMING ORGANIZATION NAME(S) AND ADDRESS(ES)
NASA Dryden Flight Research Center
P.O. Box 273
Edwards, California 93523-0273

8. PERFORMING ORGANIZATION REPORT NUMBER
H-2624

9. SPONSORING/MONITORING AGENCY NAME(S) AND ADDRESS(ES)
National Aeronautics and Space Administration
Washington, DC 20546-0001

10. SPONSORING/MONITOR'S ACRONYM(S)
NASA

11. SPONSORING/MONITORING REPORT NUMBER
NASA/TP-2006-213676

12. DISTRIBUTION/AVAILABILITY STATEMENT
Unclassified -- Unlimited
Subject Category 39 Availability: NASA CASI (301) 621-0390
Distribution: Standard

13. SUPPLEMENTARY NOTES

14. ABSTRACT
The previously developed Ko closed-form aging theory has been reformulated into a more compact mathematical form for easier application. A new equivalent loading theory and empirical loading theories have also been developed and incorporated into the revised Ko aging theory for the prediction of a safe operational life of airborne failure-critical structural components. The new set of aging and loading theories were applied to predict the safe number of flights for the B-52B aircraft to carry a launch vehicle, the structural life of critical components consumed by load excursion to proof load value, and the ground-sitting life of B-52B pylon failure-critical structural components. A special life prediction method was developed for the preflight predictions of operational life of failure-critical structural components of the B-52H pylon system, for which no flight data are available.

15. SUBJECT TERMS
Empirical loading theory, Equivalent crack-growth theory, ESE critical stress points, Operational flight-life theory, Stress load coefficients

16. SECURITY CLASSIFICATION OF: a. REPORT	b. ABSTRACT	c. THIS PAGE	17. LIMITATION OF ABSTRACT	18. NUMBER OF PAGES	19a. NAME OF RESPONSIBLE PERSON
					STI Help Desk (email: help@sti.nasa.gov)
					19b. TELEPHONE NUMBER *(Include area code)*
U	U	U	UU	60	(301) 621-0390